

## ARTICLE



# Immunohistological study of the density and distribution of human penile neural tissue: gradient hypothesis

Alfonso Cepeda-Emiliani <sup>1</sup>✉, Marina Gándara-Cortés <sup>1,2</sup>, María Otero-Alén <sup>3</sup>, Heidy García <sup>4</sup>, Juan Suárez-Quintanilla<sup>1</sup>, Tomás García-Caballero <sup>1,2</sup>, Rosalía Gallego <sup>1</sup> and Lucía García-Caballero <sup>1</sup>

© The Author(s), under exclusive licence to Springer Nature Limited 2022

Immunohistological patterns of density and distribution of neural tissue in the human penis, including the prepuce, are not fully characterized, and effects of circumcision (partial or total removal of the penile prepuce) on penile sexual sensation are controversial. This study analyzed extra- and intracavernosal innervation patterns on the main penile axes using formalin-fixed, paraffin-embedded human adult and fetal penile tissues, single- and double-staining immunohistochemistry and a variety of neural and non-neural markers, with a special emphasis on the prepuce and potential sexual effects of circumcision. Immunohistochemical profiles of neural structures were determined and the most detailed immunohistological characterizations to date of preputial nerve supply are provided. The penile prepuce has a highly organized, dense, afferent innervation pattern that is manifest early in fetal development. Autonomically, it receives noradrenergic sympathetic and nitrergic parasympathetic innervation. Cholinergic nerves are also present. We observed cutaneous and subcutaneous neural density distribution biases across our specimens towards the ventral prepuce, including a region corresponding in the adult anatomical position (penis erect) to the distal third of the ventral penile aspect. We also describe a concept of innervation gradients across the longitudinal and transverse penile axes. Results are discussed in relation to the specialized literature. An argument is made that neuroanatomic substrates underlying unusual permanent penile sensory disturbances post-circumcision are related to heightened neural levels in the distal third of the ventral penile aspect, which could potentially be compromised by deep incisions during circumcision.

*IJIR: Your Sexual Medicine Journal*; <https://doi.org/10.1038/s41443-022-00561-9>

## INTRODUCTION

Penile afferent input is required for male sexual function, providing the afferent drive for spinal reflexes that modulate erection [1]. However, types and quantities of penile nerve formations and their anatomical positions remain understudied. Historically [2–4], penile circumcision has been proposed in specialized and lay sources to both improve and impair male sexual function along various dimensions. Some contemporary literature [5–10] has suggested potential detrimental effects of circumcision in a subgroup of men in parameters such as erectile function, sensation, masturbatory pleasure, orgasm, and sexual satisfaction. Other studies [11–13] have documented severe distress of a subpopulation of men (representativeness unknown) in relation to their infant circumcisions, including reports of chronic glans insensitivity, delayed ejaculation, and unpleasant sensations (e.g., pain, numbness). The evidence regarding all these claims is contentious and contradictory [14–18], and precise neural mechanisms have not been postulated. More detailed knowledge of penile anatomy, innervation, and structure may thus contribute to our understanding of these phenomena.

Accordingly, in this paper we present detailed immunohistochemical analyses of penile innervation motivated by the idea that such knowledge might provide insight into the anatomical basis of

potential negative impacts of circumcision on male sexual function. We propose that penile innervation patterns and variations in circumcision technique (including type and extent of tissue removal, depth of incisions, etc.) likely factor into such potential outcomes. At the same time, there are shared interindividual penile (including preputial) features that bear on the range and magnitude of certain risks irrespective of circumcision technique. We also take the opportunity to explore penile neurohistology in its own right and not just in relation to circumcision.

Although circumcision is the most globally distributed genital modification, practiced in the most varied sociocultural (medicalised and non-medicalised) contexts, there continues to be a lack of understanding of preputial anatomy and physiology among medical practitioners [19–21] (Fig. 1). It has been reported based on macroscopic dissections that ~50% of dorsal nerve fibers are destined to innervate the prepuce [22], a possibly overstated estimation, but adult penile sagittal histological sections [23] have shown that dorsal nerve branches entering the prepuce are indeed substantial.

## Gradient hypothesis: a brief review of the literature

The human pendulous penis is an organ with two main axes, a major or longitudinal axis and a minor or transverse axis. It also has

<sup>1</sup>Department of Morphological Sciences, School of Medicine and Dentistry, University of Santiago de Compostela, Santiago de Compostela, Spain. <sup>2</sup>Department of Pathology, University Clinical Hospital, Santiago de Compostela, Spain. <sup>3</sup>Health Research Institute of Santiago (IDIS), Santiago de Compostela, Spain. <sup>4</sup>National Institute of Legal Medicine and Forensic Sciences of Colombia, Barranquilla, Colombia. ✉email: [alfonsomario.cepeda@rai.usc.es](mailto:alfonsomario.cepeda@rai.usc.es)

Received: 8 July 2021 Revised: 3 March 2022 Accepted: 8 March 2022

Published online: 02 May 2022

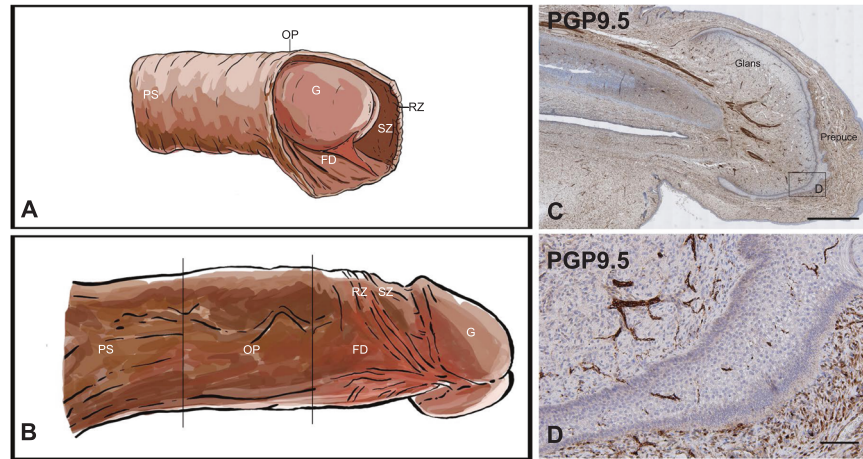


**Fig. 1 What is the prepuce?** Conventionally, it is defined as a cutaneous or mucocutaneous tissue that partially or totally covers the glans during flaccidity (A). In this standard usage, the term “prepuce” is implicitly used as a physiological descriptor of a position (covering the glans) of the distal region of the penile integument. “Prepuce” in conventional usage is not an anatomical descriptor of a discrete structure as its proximal outer limits are undefined, being directly continuous with the proximal shaft skin. This macroscopic observation is verified in fetal and adult penile sagittal histological sections. As a descriptive science anatomy uses terms of relationship and comparison (proximal, medial, superficial, etc.), terms of laterality (ipsilateral, contralateral) and terms of movement (flexion, abduction, rotation, etc.) [94]. In this conception, the term “prepuce” belongs to a category of positional terms, like “fist” or “lap”, which describe specific temporary arrangements of dynamic or mobile body parts. In the classical anatomical position, the penis is erect [94]. When retracted in this position, as appears in B and in the Rouvière and Delmas classical anatomy textbook [107], the prepuce commonly reveals four more or less well-defined regions [57, 85, 108]: (i) a smooth zone (SZ), located dorsolaterally between the glans (G) distally and the ridged zone proximally; (ii) a ridged zone (RZ), located dorsolaterally between the SZ distally and the outer prepuce proximally; (iii) a frenular delta (FD), located ventrally medial to the oblique borders of the RZ and distal to the outer prepuce; (iv) the outer prepuce (OP), located proximal to the RZ and FD, and directly continuous with the proximal shaft skin (PS). SZ, RZ and FD are three regions of the inner prepuce, the OP being the fourth region of the whole preputial structure. Note the positions of these regions in (A). Some urology textbooks contain vague references to the FD, such as “the V of the frenulum” [109] or “the frenulum, a pyramidal structure” [110], but never a formal anatomical description insisting on spatial relationships with adjacent tissues. Due to its triangular shape and proximity to the frenulum, the term frenular delta [108] was coined for this region of the inner prepuce. As the RZ is continuous with the frenulum, some [111, 112] have referred to it also as the frenar band. In this model of preputial anatomy, the SZ of the inner prepuce extends from the ridged zone to the inferior border of the corona and is thus identical to what has traditionally been denominated the “coronal sulcus”, “balanopreputial sulcus” or “neck of the glans”. In fact, the tissue between the circumcision scar line and glans is commonly referred to as inner preputial skin. This model may represent a basic pattern of preputial anatomy around which many normal variations in the definition, prominence, shape, and exact location of the regions are expected. If the penile body is divided (vertical lines in B) longitudinally in three regions of equal sizes, the distal third of the ventral aspect (i.e., the region of the ventral prepuce) has attracted attention [108] due to its putative dense somatosensory nerve supply that favors acute perception of sexual sensation. Histologically the prepuce is pentalaminar tissue [57, 82], consisting of epidermis, dermis, dartos, lamina propria and inner preputial epithelium. Each histological level has its characteristic microscopic internal organization and immunohistochemical features. During fetal development, the inner prepuce and glans are fused by sharing a common epithelium, which is innervated (C, D). This temporary squamous epithelial interface is the anlage or primordium of the preputial sac (a potential space) and has been denominated the “epithelial plate” [82], “preputial lamina” [31] or “glandopreputial lamella” [81], among other terms. We will use the term “glandopreputial common epithelium” to emphasize its epithelial nature and position as an interface shared by glans and prepuce. C is a sagittally sectioned fetal penis at 21 weeks fertilization age immunostained with PGP9.5 and D is a higher magnification of the rectangle in (C) showing PGP9.5+ intraepithelial fibers in the glandopreputial common epithelium. Preputial postnatal development consists of the gradual luminization of this epithelial interface culminating over the years in a retractile prepuce [57]. The statistical frequency and individual extent of physiological phimosis are thus inversely proportional to age, and the process of separation is usually completed by the end of puberty or earlier [57]. Scale bars: 1 mm (C), 100 µm (D).

oblique axes inclined in multiple directions according to the sectional plane, intersecting the major and minor axes at non-right angles. Morphological, neurophysiological, and psychophysical evidence suggests neurohistological patterns of density and distribution structured as gradients along the main penile axes. Cumulatively, the studies described next suggest intraindividual spatial variations of penile neural tissue quantity and functional type depending upon the anatomical position within the organ. This patterning implies consistent interindividual microscopic features of penile neural design that have been insufficiently explored in the scientific literature. Consider the following evidence:

(i) Histologically the glans, coronal sulcus and preputial integuments are one continuous tissue compartment. Winkelmann [24] reported higher densities of penile mucocutaneous end-organs distally in the coronal sulcus and their reduction proximally where hair follicles appear, but provided no quantifications. (ii) Pérez-Casas et al. [25] identified longitudinal nerve plexuses running the entire length of the penis in 20 adult

cadavers, more abundant distally in the preputial dermis. (iii) Moldwin and Valderrama [26] quantified in 35 normal preputial specimens disproportionately high nerve bundle levels ventrally, less laterally and lower dorsally. (iv) Malkoc et al. [27] counted more nerve fascicles in the distal prepuce, as opposed to the middle and proximal prepuce in 20 specimens. (v) Diallo et al. [28] described in five fresh intact cadavers higher sensory innervation in the distal third of the extra-albugineal penile compartment and reduced proximal afferent supply, ventrolateral dorsal nerve projections being greater at the frenular level. In contrast, autonomic nitrergic and noradrenergic intracavernous innervation was higher proximally and lower distally. Furthermore, Diallo et al. [28] found a higher density of afferent intracavernous nerve fibers (PMP22+) distally and lower proximally, adding another inversion of nerve class repartition across the longitudinal axis. (vi) Jang et al. [23] presented sagittal penile microsections displaying dense ventrodorsal subcutaneous S100+ nerves, with higher densities than dorsal glans innervation. (vii) Flochlay et al. [29]

noted higher concentrations of free nerve endings (FNEs) in frenular areas of two fresh complete penile specimens, and (viii) Halata and Munger [30] found so-called genital corpuscles more numerous in the frenular area and corona in seven glans specimens. (ix) Cunha et al. [31] studying 30 fetal penile specimens reported a very dense array of ventral nerves in frenular and preputial mesenchymes at 14 weeks post-fertilization. (x) Kuhn [32] described the frenular area and corona as neurologically distinct, low-threshold regions for inducing erection and ejaculation in Second World War spinal cord-injured patients, implicating sensory inflow from particularly these regions in neural pathways mediating reflexogenic erection and ejaculation. Sperm retrieval in these patients is now frequently accomplished with vibratory stimulation of the frenular area [33], but self-reported [34] and Kuhn's [32] data suggest erection and ejaculation can be achieved by more physiological stimuli, such as manual stimulation. (xi) Finally, Bossio et al. [35] documented lower fine touch sensory thresholds in the prepuce and higher in the mid-shaft, replicating results by Sorrells et al. [36].

As noted, these studies suggest that the density and functional types of penile neural tissue change according to anatomical regions. Taking as a point of reference Fig. 1B, these studies suggest that the extracavernosal somatosensory nerve supply to the penile body is concentrated distally, and in the distal sector it is more abundant ventrally, and the concentration of microscopic neural tissue decreases elsewhere in the penile body. Intracavernosally, one study [28] suggested that autonomic nerve density is higher proximally, with a greater density of visceral afferent nerves distally. Data also suggest a non-random neural organization of glanular terminal innervation, with corpuscular formations concentrated along the corona and FNEs in almost every dermal papilla, the ratio of FNEs to sensory corpuscles being approximately 10:1 [30]. Other little explored aspects of human penile innervation include immunohistochemical profiles of sensory corpuscles [37], knowledge of which has lagged compared to research on protein profiles of extra-genital corpuscles, which has undergone major advances in recent years [38], incorporating structural data of mechanotransducer proteins in mechanoreceptors [39].

As noted, permanent altered penile sensation experienced as detrimental to sexual functioning is a reported effect of circumcision [5–7, 9, 10, 40]. Note that these studies refer to adult circumcision. However, the precise causal mechanism of such altered sensation is poorly understood. It is not yet known whether this complaint is primarily organically based (that is, directly caused by acute physical effects of circumcision, such as interrupted neural pathways), and this merits thorough investigation. Nevertheless, deeper insight into the etiopathogenesis of altered penile sensation may shed light on this or other potential effects of circumcision across age groups including early childhood. Theoretically, any reduction of penile sensory capacity exceeding an unknown margin of safety could negatively impact sexual sensation and function by critically interrupting afferent pathways of sexual reflexes. The distal ventral penile aspect (Fig. 1B) is a region of special interest for being a highly erogenous [9, 41], well-defined zone for generating sexual reflexes, as evidenced by clinical observations in spinal cord-injured men [32, 33]. Although chronic supraspinal descending serotonergic disinhibition can facilitate erection in these patients by augmentation of penile reflexes [42], the local, tissular causes of this phenomenon and their implications for normal erectile physiology have not been adequately explored. The exact vascular anatomy of this region remains elusive but it is highly vascularized, sometimes causing profuse bleeding during circumcision and potential difficulties in hemostatic management [43]. This anatomical region of triangular configuration (the frenulum usually retracts into a V or inverted Y) was recently suggested [23] to be a zone of vulnerability to sensory nerve injury secondary to deep ventral incisions due to its specially dense subcutaneous

innervation. The perineal nerve innervates this zone with sensory and autonomic fibers [29, 44–46], providing an independent neural pathway for penile reflexes [47], but it can also receive ventrolateral contributions from the dorsal nerve [48, 49].

The primary aims of this study were to semiquantitatively assess the density and distribution of cutaneous and subcutaneous neural tissue on the main axes of the human adult and fetal penis, to determine if there are neural substrates in the penile structure that could substantiate claims of potential negative effects of circumcision on penile sexual sensation, given tissue resections and incisions of variable depths and trajectories. Immunohistochemical profiles of corpuscular receptors and preputial nerves were also characterized, and fetal intracavernous nitrergic neural density distribution was assessed.

## MATERIALS AND METHODS

The study was conducted in accordance with Spanish law and the 1964 Helsinki Declaration and its later amendments with approval by the Santiago-Lugo Research Ethics Committee (code 2021/179).

### Fetal specimens

Ten sagittally sectioned normal fetal penile specimens of fertilization ages ranging approximately from 14 to 30 weeks (mean 19.5, SD 4.6) were collected without patient identifiers from the Pathology Department of University Clinical Hospital of Santiago de Compostela. Fetal age was estimated using foot length measurements dated from the estimated time of fertilization [50]. Macroscopic observations of the fetuses revealed no evidence of gross caudal abnormalities.

### Adult preputial specimens

Ten fresh preputial specimens with ventral sutures were also obtained post-circumcision from the Urology Service of University Clinical Hospital of Santiago de Compostela. The mean age of patients was 27.7 years (range 18–68, SD 14.1). Some specimens were dissected transversely to visualize the complete preputial structure in the *in situ* orientation and some were further dissected into smaller pieces according to anatomical regions (ventral, dorsal, lateral). The exact medical indications for the circumcisions were unknown to us. Three specimens showed varying degrees of focal inflammation (consistent with balanoposthitis) that did not impede evaluation of the innervation. The rest were histologically normal, although phimosis could not be excluded. Written informed consent was obtained from all patients.

### Cadaveric specimens

In addition, samples were obtained from the dorsal and ventral aspects of the proximal (2 cm distal to penoscrotal and pubopenile junctions) and distal (frenular delta and adjacent zones ventrally, and frenar band and adjacent zones dorsally) penile skin regions of three intact (not circumcised) cadavers of 60, 73 and 80 years of age donated to the Faculty of Medicine of University of Santiago de Compostela for education and research. Causes of death were unknown but no penile pathologies were evident upon macroscopic observation.

### Single- and double-staining immunohistochemistry

Preputial and fetal specimens were fixed in 10% neutral buffered formalin for 24–48 h and donated cadavers were fixed by arterial perfusion also with 10% formalin. The time elapsed from surgical removal of preputial specimens to fixation was a matter of minutes. All samples were routinely processed and embedded in paraffin. Four- $\mu$ m-thick serial sections were mounted on FLEX IHC slides (Dako-Agilent, Glostrup, Denmark), stained with hematoxylin and eosin (HE), Masson's trichrome (MT) and immunostained using automated stainers (AutostainerLink 48, Dako-Agilent, Glostrup, Denmark; Dako Omnis, Agilent, Santa Clara, CA, USA) and Dako EnVision FLEX detection system following the manufacturer's instructions with the primary antibodies detailed in Table 1. Most formalin-fixed, paraffin-embedded tissue blocks were exhausted with every 11th–12th section stained with HE and MT for structural identification and intervening sections immunolabelled with axonal (NF, PGP9.5 and NSE) and Schwann cell (S100 and CD56 [neural cell adhesion molecule]) markers. Single and double immunohistochemistry with the rest of our antibody panel was used in selected slides to reveal immunohistochemical profiles of neural structures

**Table 1.** Antibodies and incubation protocols used in this study.

Antibody (clone)	Origin	Source	Code	Concentration	HIER pH	Time/temperature
$\alpha$ -SMA (1A4)	Mouse	Dako <sup>a</sup>	IR611	Prediluted	High pH	20 min/RT
Bcl-2 (124) <sup>h</sup>	Mouse	Dako <sup>a</sup>	IR614	Prediluted	High pH	20 min/RT
CD3 <sup>h</sup>	Rabbit	Dako <sup>a</sup>	IR503	Prediluted	High pH	20 min/RT
CD34 (QBEnd 10) <sup>h</sup>	Mouse	Dako <sup>a</sup>	IR632	Prediluted	High pH	30 min/RT
CD56 (123C3) <sup>i</sup>	Mouse	Dako <sup>a</sup>	IR628	Prediluted	High pH	40 min/RT
CD68 (PG-M1) <sup>h</sup>	Mouse	Dako <sup>a</sup>	IR613	Prediluted	High pH	20 min/RT
CK20 (K <sub>5</sub> -20.8) <sup>h</sup>	Mouse	Dako <sup>a</sup>	IR777	Prediluted	High pH	20 min/RT
COL-IV (CIV22) <sup>i</sup>	Mouse	Dako <sup>a</sup>	M0785	Prediluted	High pH	20 min/RT
EMA (E29) <sup>h</sup>	Mouse	Dako <sup>a</sup>	IR629	Prediluted	High pH	20 min/RT
Glut-1 (SPM498) <sup>h</sup>	Mouse	Biocare Medical <sup>b</sup>	CM 408 A, B	1:100	High pH	30 min/RT
Nestin (EPR1301(2)) <sup>h</sup>	Rabbit	Abcam <sup>c</sup>	ab176571	1:1000	Low pH	20 min/RT
NF (2F11)	Mouse	Dako <sup>a</sup>	IR607	Prediluted	High pH	20 min/RT
nNOS (C7D7) <sup>i</sup>	Rabbit	Cell Signaling Technology <sup>d</sup>	4231	1:50	High pH	24 h/4 °C
NSE (BBS/NC/VI-H14) <sup>i</sup>	Mouse	Dako <sup>a</sup>	IR612	Prediluted	High pH	30 min/RT
Pan-TRK (EPR17341) <sup>j</sup>	Rabbit	Roche/Ventana <sup>e</sup>	790–7026	Prediluted	High pH	32 min/37 °C
PGP9.5	Rabbit	Cell Marque <sup>f</sup>	CMC31811040	Prediluted	High pH	30 min/RT
Piezo2 <sup>h</sup>	Rabbit	Sigma-Aldrich <sup>g</sup>	HPA031974	1:1000	Low pH	24 h/4 °C
S100	Rabbit	Dako <sup>a</sup>	IR504	Prediluted	High pH	30 min/RT
SOX10 (BC34) <sup>h,i</sup>	Mouse	Biocare Medical <sup>b</sup>	ACI3099C	1:100	High pH	30 min/RT
TH (E2L6M) <sup>i</sup>	Rabbit	Cell Signaling Technology <sup>d</sup>	58844	1:50	High pH	24 h/4 °C
VACHT (S6–38) <sup>h</sup>	Mouse	Sigma-Aldrich <sup>g</sup>	SAB5200241	1:100	High pH	24 h/4 °C
Vimentin (V9) <sup>h</sup>	Mouse	Dako <sup>a</sup>	IR630	Prediluted	High pH	20 min/RT

The reader is referred to Chetty et al. [100], Smoller [101], True [102] and Gratzl and Langley [64] for brief backgrounds on these antibodies. For pan-TRK, nestin, nNOS and VACHT see references [103–106].

$\alpha$ -SMA  $\alpha$ -smooth muscle actin, Bcl-2 B-cell lymphoma 2, CD cluster of differentiation, CK20 cytokeratin 20, COL-IV collagen type IV, EMA epithelial membrane antigen, Glut-1 glucose transporter 1, NF neurofilament, nNOS neuronal nitric oxide synthase, NSE neuron-specific enolase, Pan-TRK pan-tropomyosin receptor kinase, PGP9.5 protein gene product 9.5, SOX10 Sry-related HMG-box 10, TH tyrosine hydroxylase, VACHT vesicular acetylcholine transporter, HIER heat-induced epitope retrieval, RT room temperature.

<sup>a</sup>Glostrup, Denmark; <sup>b</sup>Pacheco, CA, USA; <sup>c</sup>Cambridge, UK; <sup>d</sup>Beverly, MA, USA; <sup>e</sup>Mannheim, Germany; <sup>f</sup>Rocklin, CA, USA; <sup>g</sup>Saint Louis, MS, USA.

<sup>h</sup>These antibodies were used exclusively on adult and cadaveric specimens, while the rest were used on all specimen types.

<sup>i</sup>These antibodies involved an additional signal amplification step by incubation with EnVision FLEX+ Mouse/Rabbit Linker (Dako) for 15 min.

<sup>j</sup>Pan-TRK immunostains were performed with the Benchmark Ultra platform (Ventana Medical Systems, Tucson, AZ, USA) and the OptiView DAB Detection Kit following the manufacturer's instructions. The antibody detects an epitope conserved across TRK proteins A, B and C in their C-terminal regions [103].

and other immunohistological features of interest. Tissue antigens were visualized with EnVision FLEX/HRP diaminobenzidine (Dako-Agilent) and EnVision FLEX/HRP magenta (Dako-Agilent) chromogen solutions.

Double staining with CD34 (a marker of endoneurial fibroblasts) and NF, S100 or CD56 was used to reveal endoneurial and neural components of corpuscular receptors in the same section. nNOS, VACHT and TH were used for the identification of autonomic nitrergic (parasympathetic), cholinergic (parasympathetic) and noradrenergic (sympathetic) fibers, respectively. EMA and Glut-1 were used to stain perineurial fibroblasts, COL-IV to detect basal laminae, CK20 to identify Merkel cells and SOX10 (a Schwann cell lineage marker) for nuclear staining of Schwann cells. Preputial smooth muscle was immunostained with  $\alpha$ -SMA. Intermediate filament types in mechanoreceptors were immunodetected with NF, vimentin, nestin (a neural stem cell marker) and  $\alpha$ -SMA. Anti-apoptotic proteins were investigated with a Bcl-2 antibody. Neurotrophin high-affinity receptors were revealed with a pan-TRK marker. Piezo2 (an ion channel with mechanotransducer properties in vertebrates) axonal expression was recently described in human preputial [37] and clitoral [51] corpuscular receptors, and we used a Piezo2 antibody to detect penile mechanoproteins. Finally, expression of the macrophage-associated antigen CD68 and the pan-T cell antigen CD3 in Pacinian corpuscles was explored.

Slides were observed and photographed in an Olympus BX51 microscope (Tokyo, Japan) equipped with a digital camera (Olympus DP70, Tokyo, Japan). Low-magnification images of preputial and fetal sections were taken with a Leica DMD108 digital microscope (Wetzlar, Germany) and the scanner used for quantifications. Brightness, contrast, and other minimal adjustments of microphotographs were made using Adobe Photoshop CS5 (San Jose, CA, USA).

## Quantifications

After detailed scrutiny of most of the tissue per paraffin block, nerve bundle regional densities were initially evaluated as follows: absence (–), low (+), moderate (++) , high (+++). Next, four representative sections with the highest nerve densities from each region of preputial and cadaveric specimens were scanned with a PathScan Combi digital pathology scanner (Excilone, Elancourt, France) and S100+ nerve bundle profiles were manually counted by two independent observers in  $\geq 4$  randomly selected neural hotspots of 1 mm<sup>2</sup> each per slide. Fetal intracavernous nNOS+ nerves were identically counted in proximal, intermediate, and distal regions. Non-fetal slides were codified and blinded prior to all analyses and unblinded to review results. Neural densities are presented as mean/mm<sup>2</sup>  $\pm$  SD. We aimed to provide numerical data on what we typically found on these sections, but no further statistical analyses were conducted.

## RESULTS

### Fetal specimens

Preputial nerves were CD56+, S100+, NF+, NSE+, PGP9.5+, pan-TRK+, nNOS+ and TH+. The nerves in the glans corpus spongiosum shared this immunohistochemical profile. Subcutaneous preputial neural densities were higher ventrally, at mid-frenular levels and near the midline, as opposed to dorsal and lateral penile aspects (Fig. 2). Some of the preputial nerves were distal continuations of nerves traveling superficial to Buck's fascia but numerous subcoronal branches of dorsal, perineal, and ventral intraspongiosal nerves to

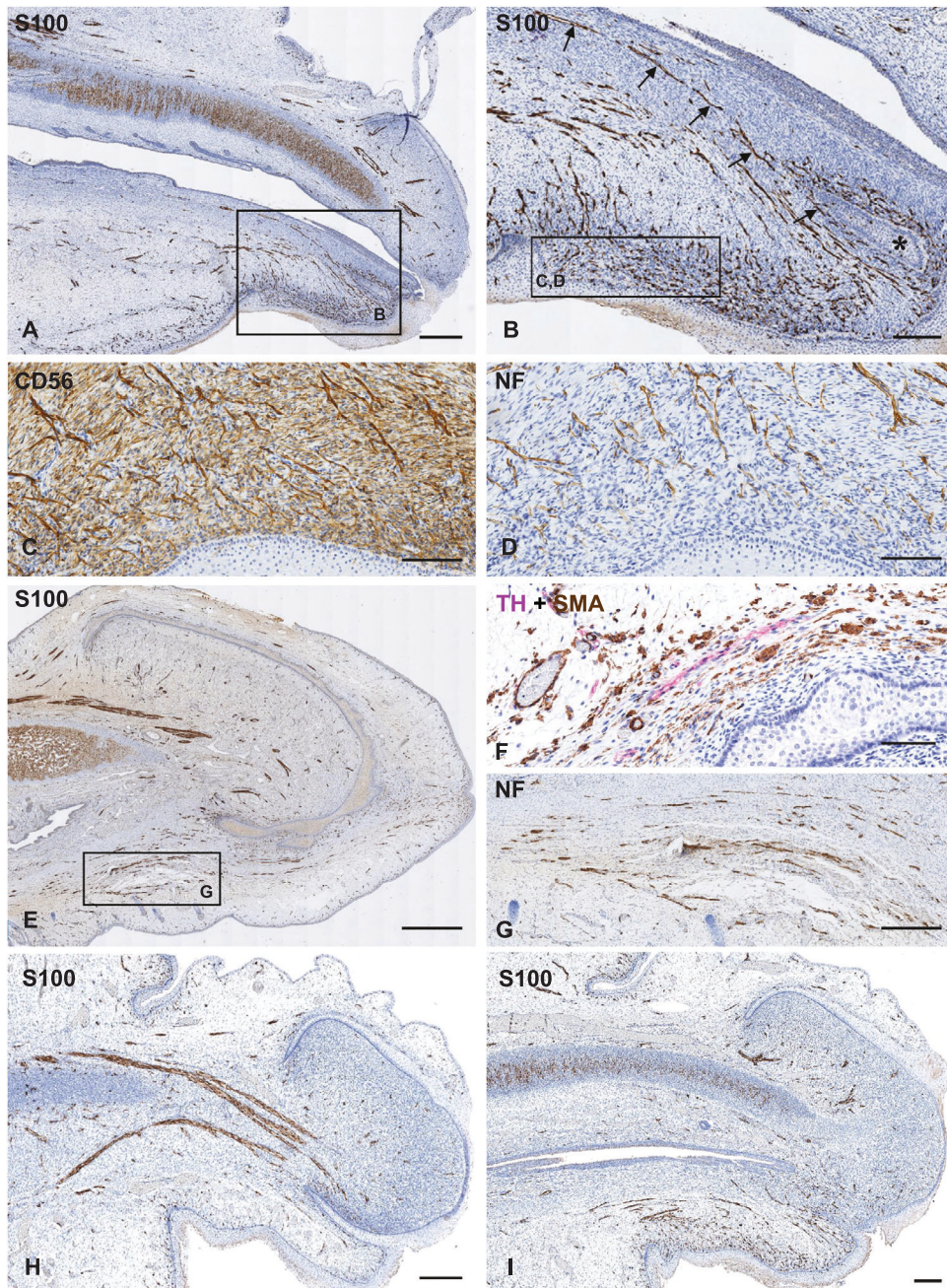
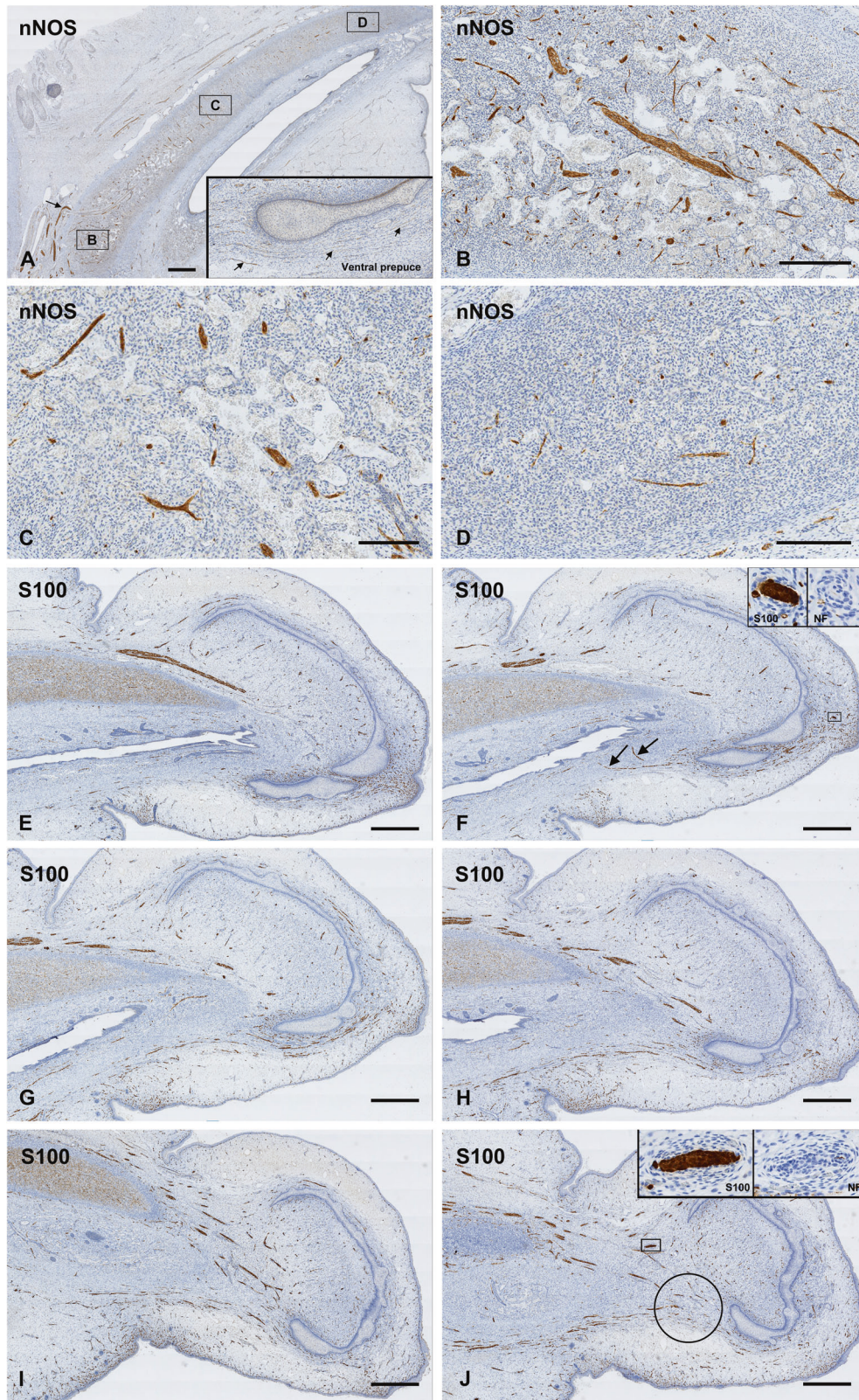


**Fig. 2** Ventral-dorsal innervation patterns in four sagittally sectioned human fetal penile specimens. 16 (A–D), (H, I), 23 (E, G) and 21 (F) weeks post-fertilization. (A, E, H, I) are low-magnification images for general overviews of the sections, all displaying greater ventral subcutaneous S100+ nerve densities. The strand of tissue in the upper right corner of (A) is artifactual but the ventral preputial epithelium of this specimen was very much thicker than the dorsal preputial epithelium. C, D are higher magnification images of serial sections 26  $\mu\text{m}$  apart from the correspondent rectangle in (B), showing these nerve arrays immunostained for CD56 and NF. In B, note the ventral glandopreputial common epithelium tangentially sectioned (asterisk) and intraspungiosal fibers (arrows) reaching the glans underside, like fibers in Fig. 3F. In C, note CD56 immunopositivity in the preputial mesenchyme, indicating developmental CD56 upregulation, consistent with the well-known functions of this molecule in neuronal development [64]. Upon closer inspection, some minute intraepithelial fibers are seen. F shows TH+ nerves (magenta) entering the dorsal prepuce of a 21-week specimen, surrounded by  $\alpha\text{-SMA}$ + dartos smooth muscle (brown). G is a higher magnification image of a serial section 1  $\mu\text{m}$  apart from the correspondent rectangle in (E), showing numerous NF+ thin nerves in the glans underside. H is a low-magnification image of a fetal penis at 16 weeks with dual glans innervation by S100+ dorsal nerves and a thick ventral perineal nerve trunk, comparable in size to the dorsal nerves. The ventral preputial epithelium is much thicker than the dorsal preputial epithelium, and serial sections in this specimen revealed toward the midline (I) a ventral-dorsal innervation pattern with higher ventral density identical to that of (A). Nevertheless, in H, the presence of profuse perineal nerve ramifications innervating the ventral prepuce can be appreciated on careful observation, although these branches have mostly fallen out of the plane of section. A rich interanastomosing nerve network is similarly appreciated in (H) between the dorsal and perineal thick nerve trunks. Scale bars: 0.4 mm (A), 0.2 mm (B), 150  $\mu\text{m}$  (C, D), 0.8 mm (E), 100  $\mu\text{m}$  (F), 400  $\mu\text{m}$  (G), 0.2 mm (H, I).



superficial levels were observed. Conversely, the main dorsal nerve axonal population innervated the glans in every specimen (as expected), but in a particularly fortuitous section of one specimen, a thick perineal nerve trunk lateral to the urethra also innervated the ventral glans aspect (Fig. 2H). The glans was also innervated by

thinner fibers located in the ventral aspect of the corpora cavernosa, by thin intraspongiosal fibers coursing longitudinally through the corpus spongiosum, and by much thinner fibers that coursed longitudinally in contact with the dorsal tunica albuginea underneath the main trunks of the dorsal nerves and the vasculature.

**Fig. 3** Intra and extracavernosal innervation patterns in sagittal sections of two human fetal penile specimens. 20 (A–D) and 21 (E–J) weeks post-fertilization. **A, E–J** are low-magnification images for general overviews of the sections. **B–D** are higher magnifications of a section 42  $\mu\text{m}$  apart from the same specimen and regions of the correspondent rectangles in **(A)**. **A–D** show an intracavernosal proximodistal gradient of nNOS+ fiber density and size, with higher quantities and sizes in proximal **(B)** compared to intermediate **(C)** and distal **(D)** regions. While not so visually pronounced in some specimens, a consistent tendency toward decreased distal autonomic nerve density was nevertheless detected. nNOS intra and extracavernosal staining intensities were also highest proximally and lower distally. Sinusoidal spaces were larger proximally and centrally and reduced distally and peripherally. In **A**, note a large blood vessel perforating the proximal tunica albuginea escorted by a nNOS+ nerve branch (arrow). Inset in **A** shows nNOS+ fibers entering the ventral prepuce of the same section at higher magnification. **E–J** As S100+ nerves were followed from midline to lateral in these sections 42  $\mu\text{m}$  apart from each other, a convergence (circle in **J**) was noted laterally near the glans underside between descending dorsal and longitudinal perineal nerves. In **F**, note intraspongiosal nerves (arrows) also reaching this region and in **(E)** note a neural density in the ventral prepuce. Insets in **F, J** are higher magnifications of the correspondent squares displaying S100+ and NF+ serially sectioned developing Pacinian corpuscles in the preputial mesenchyme **(F)** and near the dorsal nerve **(J)**. Scale bars: 0.8 mm **(A, E–J)**, 400  $\mu\text{m}$  **(B)**, 200  $\mu\text{m}$  **(C, D)**.

Preputial nNOS and TH staining intensities were heterogenous, strong to low (mostly moderate), but represented a significant proportion of preputial nerves identified with general innervation markers. nNOS+ intracavernous nerve density was higher proximally (+++, 28.12 fibers/ $\text{mm}^2 \pm 5.84$ ) and reduced in intermediate (++, 15.37 fibers/ $\text{mm}^2 \pm 3.54$ ) and distal (+, 5.75 fibers/ $\text{mm}^2 \pm 1.83$ ) regions (Fig. 3A–D). The TH+ intracavernous nerve distribution paralleled the nitrergic pattern, but no nerve counts were made. Lateral to 7 o'clock positions descending dorsal nerve branches seemed to converge in a region near the glans underside with descending ramifications of nerves located in the ventral aspect of the corpora cavernosa, with branches of ventral intraspongiosal nerves and with direct ventral perineal nerve projections, forming a nerve convergence at this position (Fig. 3E–J). Thick and thin nNOS+, S100+, CD56+, PGP9.5+ and pan-TRK+ nerves perforating the tunica albuginea were common proximally, either associated to blood vessels or isolated. Some tended to follow ascending courses to reach the dorsal corpora cavernosa before perforating the tunica albuginea (Fig. 3A), whereas others followed descending courses. Due to their positions underneath the vasculature, their close contact with the tunica albuginea and their routes proximal to the corpora cavernosa, these nerves could be differentiated from the main trunks of the dorsal nerves which occupied a superior position closer to the pubic bone, and thus some corresponded to cavernous nerves from the pelvic plexus and others might have been dorsal nerve branches. In all specimens, the tunica albuginea of the ventral surface of the corpus spongiosum was inconspicuous to absent.

PGP9.5+ and pan-TRK+ intraepithelial fibers were present throughout all penile epithelia observed: glandopreputial fused, outer preputial, urethral, urethral glandular and scrotal epithelia, but were especially dense and eye-catching in the midline and peri-midline ventral outer prepuce at 16 weeks, with reductions laterally and proximally, as distal prolongations of very dense ventral nerves penetrating a developing COL-IV+ basal lamina (Fig. 4). Particularly at 16 weeks, intraepithelial and subepithelial preputial nerve fiber densities were directly proportional to overlying epithelial thicknesses (Figs. 2A–D, H, I and 4A). A very rich profusion of descending fan-shaped dorsal nerve branches entering the glans ended predominantly in the glans corpus spongiosum, with lower nerve densities near the glans epithelium in those specimens in which a distinct lamina propria was present. Numerous developing Pacinian corpuscles were observed through the whole course of the dorsal nerve (adjacent to the nerve) and in the scrotal and preputial mesenchyme (Fig. 3F, J).

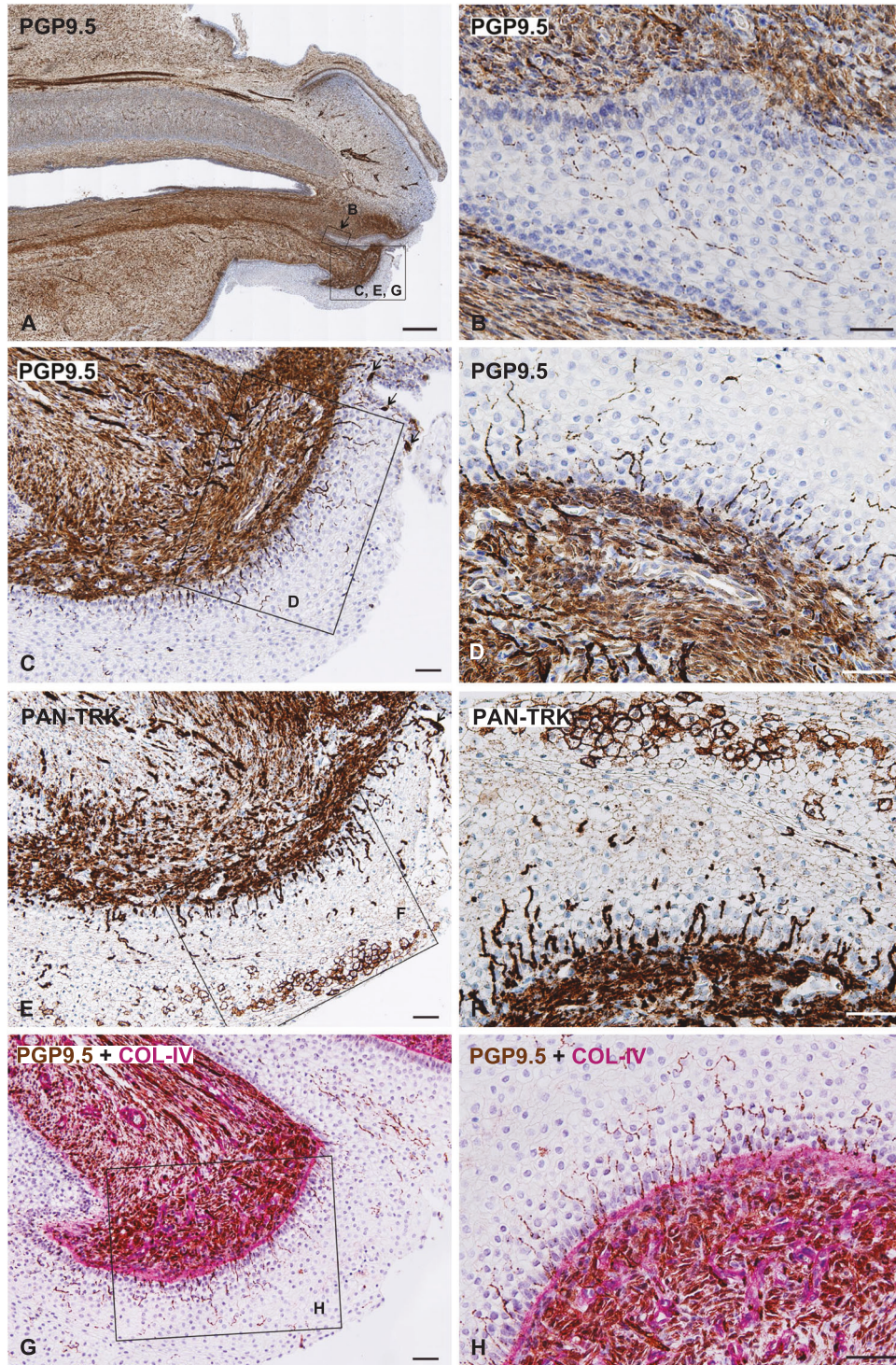
#### Adult preputial and cadaveric specimens

Axons within preputial nerve bundles were NF+, NSE+, PGP9.5+, CD56+, TH+, nNOS+ and VAcHT+ (Fig. 5). The perineurium was COL-IV+, vimentin+, EMA+, Glut-1+, and occasionally nNOS+ and  $\alpha$ -SMA+. Endoneurial fibroblasts were CD34+ and a small proportion of fibroblast-like cells were nestin+ and pan-TRK+.

Schwann cells in nerve bundles were SOX10+, S100+, CD56+, vimentin+ and COL-IV+. Other cells within nerve bundles likely corresponding to Schwann cells and/or axons were Bcl-2+, nestin+, Piezo2+ and pan-TRK+, but exact immunolocalizations of these markers could not be assured with light microscopic immunohistochemistry. nNOS and TH focal or patchy expression was seen within numerous (but not all) nerve bundles. Intensely stained vascular and dartos smooth muscle nerve profiles were widespread and dense particularly with CD56 and NSE, but nNOS+ and TH+ vascular nerves were also seen, and some nitrergic and noradrenergic fibers innervated dartos smooth muscle. Conversely, no cholinergic fibers innervated blood vessels, smooth muscle or sweat glands. Smooth muscle bundles ( $\alpha$ -SMA+) oriented in all directions comprised the central axis of the prepuce between the dermis and lamina propria, forming a most dense and intricate plexiform dartos layer embedded within a fibroelastic vascular connective tissue (Fig. 6D–K). This muscular formation was also evident in fetal specimens (Figs. 2F and 6A–C).

HE observation revealed obvious differences between nerve bundle densities of proximal and distal penile regions of cadaver specimens, and between ventral and dorsal aspects of preputial specimens. This was confirmed by immunohistochemistry, which revealed in the sampled 1  $\text{mm}^2$  neural hotspots of cadaver tissues higher densities of S100+ nerve bundles in the frenular delta (++, 11.5/ $\text{mm}^2 \pm 2.6$ ), less in the dorsal frenar band (++, 8.3/ $\text{mm}^2 \pm 2.4$ ), and exceedingly less at dorsal proximal (+, 5.2/ $\text{mm}^2 \pm 1.6$ ) and ventral proximal (+, 4.9/ $\text{mm}^2 \pm 1.6$ ) shaft (see Materials and Methods and Fig. 1 for these locations). Preputial nerve bundle densities in the sampled 1  $\text{mm}^2$  neural hotspots were higher ventrally (+++, 31.7/ $\text{mm}^2 \pm 5.4$ ) as opposed to lateral (++, 16.4/ $\text{mm}^2 \pm 4.6$ ) and dorsal (+, 9.8/ $\text{mm}^2 \pm 2.6$ ) aspects. Typical of ventral preputial sections were irregularly distributed dense aggregations of small bundles (Fig. 5D) not seen in other regions.

Corpuscular receptors consisted of Meissner, genital, Krause, Pacinian, Ruffini-like and many other nonspecific formations, with generally normal immunohistochemical profiles (Figs. 7 and 8). Schwann cells in sensory corpuscles were SOX10+, S100+, CD56+, Bcl-2+, nestin+, vimentin+ and COL-IV+. Corpuscular axons were NF+, NSE+, PGP9.5+ and pan-TRK+. When present, capsular layers of non-Pacinian corpuscles were CD34+. Glut-1+ perineurial fibroblasts were occasionally detected in non-Pacinian deep dermal formations (Fig. 7O) but together with EMA+ perineurial fibroblasts were characteristic of the outer core of Pacinian corpuscles (Fig. 8G, I). Five sections per specimen were processed for CK20 but no Merkel cells were identified. In all specimens, genital corpuscles were predominantly restricted to ventral sections. Pacinian corpuscles were observed in every specimen in the superficial or deep reticular dermis, lamina propria or dartos in all preputial regions. Clusters of three to eight papillary corpuscles were observed in adjacent fields fundamentally in the frenular delta and ventral prepuce, but isolated corpuscles could be seen everywhere. Although no counts were attempted, in any one of these sections a variety of non-Meissner



corpuscles was evident. Proximal penile skin corpuscles had the lowest densities and could not be identified in most sections of each paraffin block.

Two relations were distinct: (i) sensory receptor size was inversely related to sensory receptor densities, with FNEs most abundant (Fig. 9) and Pacinian corpuscles less numerous; and (ii) degree of corpuscular encapsulation was a function of dermal position, i.e., most papillary corpuscles were non-encapsulated or partially encapsulated, occasionally with CD34+ stromal condensations around them without forming true capsules,

whereas most corpuscles in the reticular dermis and dartos had well-delimited, variably thickened ensheathments with flattened nuclei, attaining greater thicknesses in Pacinian corpuscles. Among corpuscular receptors the most numerous were the papillary corpuscles, which morphologically included a highly variable group, among which numerous typical Meissner corpuscles were present. A continuum of intracorporeal axonal density characterized all non-Pacinian formations independent of histological position, from minimally to highly axonally branched.

**Fig. 4 PGP9.5 and pan-TRK immunoreactive intraepithelial fibers in a mid-sagittally sectioned fetal human penis at 16 weeks fertilization age.** **A** is a low-magnification image giving an overview of the section. Note the disproportionately greater preputial epithelial thickness in the ventral aspect compared to the dorsal aspect. **B** is 46  $\mu\text{m}$  apart from the same region of the correspondent rectangle in **(A)** at high magnification. **C, E, G** are sections approximately 10  $\mu\text{m}$  apart from each other from the same ventral preputial region indicated in **(A)** and **D, F, H** are higher magnifications of the correspondent rectangles in **(C, E, G)**. Single immunohistochemistry: **B** shows PGP9.5+ thin intraepithelial fibers in the ventral glandopreputial common epithelium. **C–F** show PGP9.5+ and pan-TRK+ intraepithelial fibers in the ventral outer prepuce. In upper right corner of **(C, E)** note terminal swellings or varicosities (arrows) of some fibers abutting the epithelial border. Pan-TRK+ epithelial cells with a membranous or cytoplasmic staining pattern in the higher epithelial strata of **(E, F)** and inconspicuous nerve invasion of these strata suggest these cells may sequester neurotrophins through paracrine or autocrine mechanisms perhaps modulating nerve target invasion. Non-neuronal cells in the preputial mesenchyme were also intensely pan-TRK+ and a punctate, diffuse epithelial pan-TRK immunoreaction was detected. Double immunohistochemistry: **G, H** reveal outer preputial PGP9.5+ intraepithelial fibers (brown) piercing the COL-IV+ basal lamina (magenta). Subepithelially note COL-IV+ blood vessels and perineurial collagen (both magenta), although antigen locations are not so clearly differentiated due to extensive staining of both markers and thus some chromogen overlap. In the upper right corner of **G**, note a dense cluster of fibers in the fused glandopreputial common epithelium. At higher magnifications **(B, D, F, H)**, note that these intraepithelial fibers had straightened, serpentine and interanastomosing courses, traversing epithelial intercellular spaces, cytoplasm and nuclei and ending in the lower half of the ventral preputial thickened epithelium. PGP9.5 intensely stained the fetal penile mesenchyme, more avidly in the ventral half **(A)**, indicating upregulation of this ubiquitin carboxyl-terminal hydrolase during penile morphogenesis. Scale bars: 0.4 mm **(A)**, 50  $\mu\text{m}$  **(B–H)**.

## DISCUSSION

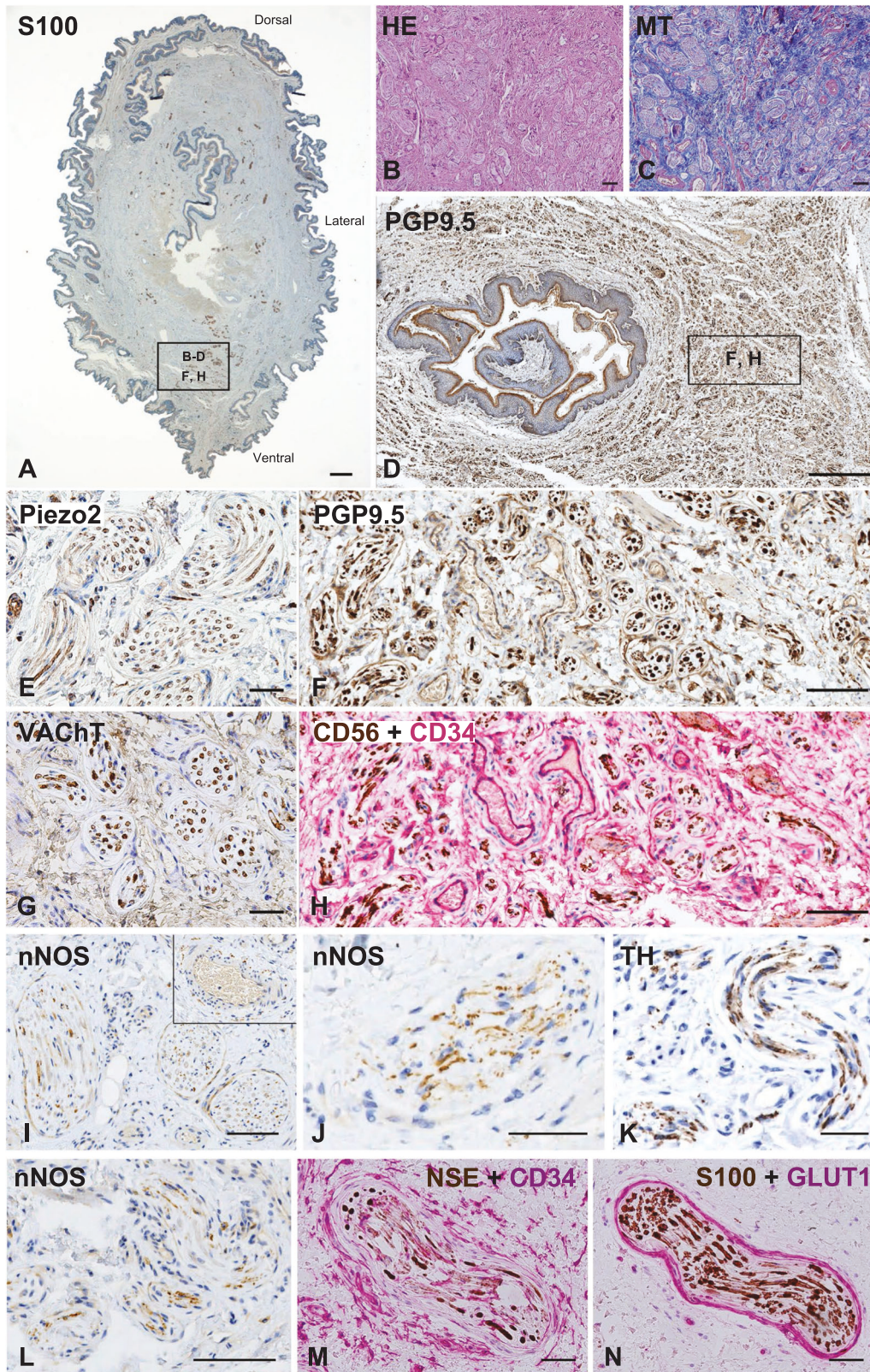
### Penile neurohistology

Comparing our results with previous literature, they generally parallel the studies discussed in our introduction and support the concept that preputial histological features of highly organized and dense neural supply differentiate it from other penile and extra-genital cutaneous tissues. We detected striking innervation biases across our fetal, preputial, and cadaveric samples towards the ventral prepuce, including a region roughly corresponding in the conventional anatomical position (penis erect) to the distal third of the ventral penile aspect. Adult corpuscular receptor, nerve bundle and fetal nerve densities were consistently higher at this level and reduced proximally. This anatomical region includes the glans underside and frenulum, which have been considered in classical [52–54] and recent literature [9, 41, 55, 56] zones of acute or heightened sexual sensation. In light of our data, the embryological base of its increased neural density seems to be a greater ventral axonal development of thin nerve fibers concurrent with lesser fasciculation (as opposed to greater dorsal fasciculation), reflected in impressive preputial PGP9.5+ and pan-TRK+ intraepithelial fibers at 16 weeks post-fertilization. These fibers were classically described by Dogiel and Ohmori (see reference [57]), denied by Winkelmann [58] and redescribed by Seto [59] using silver impregnations, but we present the first unequivocal immunohistochemical evidence of these neurohistologic entities. We have also detected profuse intraepithelial fibers in the glandopreputial common epithelium of human female fetal specimens using markers such as CD56 and NSE (unpublished data). Fetal intraspongiosal fibers apparently reaching the penile glans underside suggest a link between urethrospongiosal function and afferent input from this region. In addition, this region may be a point in which branches of all penile extracavernosal nerves tend to converge, but this requires immunohistological verification using adult penile macrosections. Large format histology will provide a better appreciation of the intricacies of penile nerve pathways.

A population of unmyelinated, low-threshold afferent C-tactile fibers is believed to mediate affective components of light touch in hairy skin but whether analogous small and/or large-fibered systems mediate penile sexual sensation remains unexplored [60]. Consistent with our results, other studies [25, 26, 61–63] have reported large numbers of unmyelinated nerves in the prepuce, both within nerve bundles and as FNEs. CD56 is commonly considered a marker of non-myelinating Schwann cells and unmyelinated fibers [64]. Its expression within all preputial nerve bundles in our study implies a substantial proportion of unmyelinated nerve traveling within these bundles. We restricted the name “genital corpuscle” to those deep dermal relatively large,

encapsulated, internally septated or lobulated formations with profuse axonal densities, similar to those recently described in the clitoris by García-Mesa et al. [51] using modern immunohistological methods; although, other nerve formations we encountered could also be included in this category. The physiological stimulus-response properties of genital corpuscles have not been characterized. Ultimately, the point at issue here concerns the peripheral neural substrates of penile erogenous sensation. Adapting a phrase by Mountcastle [65] originally used in relation to Krause corpuscles and microneurography: no variety of somatic sensation has ever been correlated in waking humans with neural activity derived from single penile mechanoreceptors. Microneurography recordings from the prepuce and glans would thus be interesting to begin to unravel this problem. Georgiadis and Kringelbach [60] note that encoding of sexual pleasure happens mostly in the brain, but the degree to which erotically experienced penile sensations are peripherally encoded is not known. A long-delayed renewed scientific impetus seems necessary to advance understanding of the afferent contribution to erectile function and of the human penis as a somatosensory organ fine-tuned for sexual sensation. It would be interesting to map the intra and extracavernosal distribution of the various known molecules [39] that are directly and indirectly responsible for mechanotransduction. Although we observed no clear-cut Piezo2 corpuscular immunopositivity, we observed Piezo2+ nerve bundles, albeit with background staining in non-neuronal tissues. Nevertheless, others [37, 51] have described Piezo2 expression in sensory corpuscles, so our antibody or incubation protocol might not have been adequate.

We have performed extensive immunohistological characterizations of human preputial innervation selectively staining the main corpuscular and nerve bundle cell types. Cold and Taylor [57] stated that most preputial corpuscular receptors are Meissner corpuscles, but we identified a broad diversity of corpuscular formations, and the non-Meissner corpuscles were not negligible in our specimens. Sensory corpuscles were often difficult to classify due to their variable and irregular morphologies. Immunohistochemical profiles of corpuscular receptors were similar to those reported for extra-genital corpuscles [38], supporting the idea [37] that their protein compositions are location-independent. CD34+ corpuscular ensheathments are thought to be [37, 38] of endoneurial origin but a telocytic nature has been defended [66], requiring further elucidation. Of course, these two capsular constituents (endoneurial fibroblasts and telocytes) need not be mutually exclusive. SOX10 nuclear expression in corpuscular lamellar cells and the knowledge that sensory corpuscles are extensions of peripheral nerve components support the glial (Schwann) lineage [67] of these cells. Pan-TRK



adult corpuscular axonal expression indicates continued responsiveness to neurotrophins, which are implicated in the maintenance of fully differentiated sensory neurons and corpuscles [68, 69].  $\alpha$ -SMA Pacinian irregular capsular positivity suggests some preputial Pacinian corpuscles may be fluid-filled contractile

structures, with  $\alpha$ -SMA unevenly distributed throughout the capsule. During the corpuscular inside-out sequence of histogenesis [70], cells with cytoplasmic  $\alpha$ -SMA might be incorporated into the Pacinian fibrous capsule from the smooth muscle-rich preputial dartos. Alternatively, these might have been cells with

**Fig. 5 Human adult preputial nerve bundles and their immunohistochemical profiles.** Nerve bundles were identified as variably sized and shaped axonal collections running together ensheathed by clearly defined and compact perineurium easily observed with HE (B) and MT (C) stains. B–D, F, H are sections from a different paraffin block from the same specimen and approximately the same region of the rectangle in (A). F is a higher magnification of the rectangle in (D) and H is serially sectioned with (F). Single immunohistochemistry: A is a low-magnification image of a transversely sectioned prepuce from a 23-year-old man showing the complete preputial structure, revealing a ventral-dorsal pattern of S100+ nerve bundle density distribution with higher ventral densities. Nerve bundles were also immunopositive for PGP9.5 (D, F), Piezo2 (E), VACHT (G), nNOS (I, J, L) and TH (K). In D, note the repletion of nerve bundles in the ventral prepuce. Inset in I, depicts autonomic cutaneous nNOS+ arteriolar nerve profiles. In I, L, contrast nNOS patchy and focal expression within these bundles with the more diffuse expression pattern in (J). Double immunohistochemistry: CD56 (brown in H) stained all preputial nerve bundles, surrounded in (H) by CD34+ dermal cells, blood vessels and smooth muscle (magenta). Serially sectioned preputial nerve bundles revealed a normal structure with CD34 expression within endoneurium (M), absence of CD34+ cells in perineurium (M), and expression of the classical perineurial marker Glut-1 (magenta in N). Scale bars: 1 mm (A), 50  $\mu$ m (B, C, E, G, J, K, M, N), 400  $\mu$ m (D), 100  $\mu$ m (F, H, I, L).

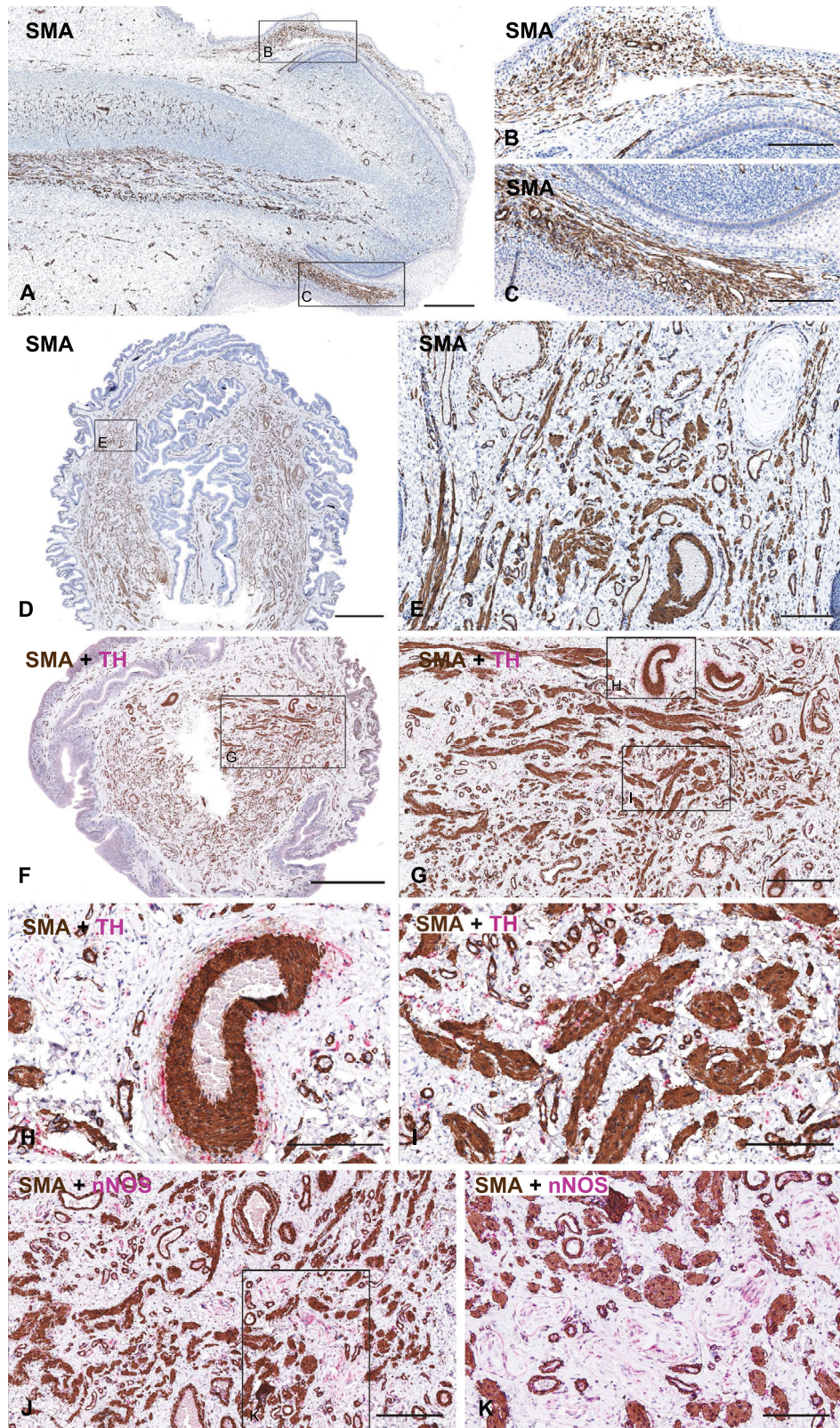
myofibroblastic differentiation. The Bcl-2 corpuscular staining patterns were suggestive of lamellar cell protein location, and functions beyond modulating apoptosis in adult corpuscles remain to be explored. Nestin corpuscular expression also indicated lamellar cell location of the protein, suggesting possible neural stem cell niches within preputial corpuscles. Nestin was also expressed within preputial nerve bundles, smooth muscle, endothelial cells, and fibroblasts/fibrocytes. These nestin+ cell populations with possible multilineage differentiation capacity [71] might open new avenues in ongoing tissue engineering efforts that aim to develop biological substitutes capable of restoring the structural and functional characteristics of the prepuce in circumcised men [72].

nNOS+ fibers have been reported in female fetal and prepubertal labial and preputial skin [73, 74], but to our knowledge male preputial nNOS+, VACHT+ and TH+ nerve bundles have not been described elsewhere. The absence of blood vessels and glandular cholinergic innervation in our study must be taken with caution as these fibers are present in mammalian skin [75, 76]. A subset of postganglionic sympathetic cutaneous fibers is cholinergic but parasympathetic nNOS+ fibers in superficial (cutaneous) histological levels may be specific to external genitalia and the nasociliary nerve [77]. Preputial innervation is thus more complex than previously acknowledged and these parasympathetic fibers should be studied in detail, as they putatively represent nNOS+ nerve fibers reaching the prepuce through caverno-pudendal hilar communicating branches [44], although a cavernous nerve-independent nNOS source cannot be ruled out. We believe that dorsal nerve branches might have been among those tunical perforating nNOS+ nerve trunks displaying ascending courses that we identified in the proximal tunica albuginea. This is supported by findings and three-dimensional reconstructions by Alsaïd et al. [78] showing that the pudendal nerve tends to follow an ascending course to reach the corpora cavernosa, whereas the cavernous nerve tends to follow a descending course. In this way, a direct motor contribution of the pudendal nerve to erection as part of supplementary pro-erectile pathways seems at least plausible. Kozacioglu et al. [79] recently presented electrophysiological and immunohistochemical evidence in a rat model of such nitrergic pathways, demonstrating an intracavernosal response to dorsal nerve electrostimulation. In a previous anatomical dissection study, Kozacioglu et al. [80] demonstrated tunical perforating dorsal nerves in 16 of 22 human adult cadavers. In our study, we also demonstrated nNOS+ nerves in the prepuce. To the extent that dorsal nerves (branches of the pudendal nerve) innervate penile skin (including the prepuce), this could, in turn, possibly lead to a reevaluation of the degree of surgical interference with penile skin that is admissible during penile surgeries, including circumcision. Due to nNOS preputial immunopositivity, a structural and physiological connection that requires further exploration may exist between penile skin and the intracavernosal compartment.

### Fetal and postnatal penile anatomy

While caution is necessary to extrapolate from fetal to adult penile morphology, previous studies [44] suggested that fetal penile neuroanatomy is reasonably comparable to that of adults. The basic architecture of the human fetal penis at 16 weeks is preserved in the adult penis. The fetal phallus at this age has yet to undergo organ growth by the uniform cellular proliferation that gradually separates the glans and prepuce from pubopenile and penoscrotal junctions lengthening the proximal shaft. However, as van der Putte [81] elegantly noted, throughout preputial formation the most proximal regions of the glandopreputial common epithelium remain fixed in relation to underlying structures such as the distal corpora cavernosa and main neurovascular elements entering the glans. We extend this observation suggesting that, once the prepuce is fully formed, during subsequent penile growth the position of the most proximal regions of the glandopreputial epithelium (and future preputial sac) also remains mostly static in relation to the overlying preputial mesenchyme and underlying distal corpora cavernosa and neurovascular structures. We believe it is the interlocking between the distal corpora cavernosa and the glans that maintains these structural relations during fetal and postnatal penile growth. Our fetal sagittal penile sections are thus a miniature version of the anatomic levels of the adult distal penis as schematized sagittally by Velazquez et al. [82]. Accordingly, that dense subcutaneous ventral fetal neuroanatomy we identified is similar to what has been described in adult penile sagittal sections [23].

By means of fetal neurohistology, we have also described the fact known to electrophysiologists [83] that the glans may have dual innervation by perineal and dorsal nerves, which may have surgical implications for glanuloplasties. Moreover, our fetal data are consistent with two immunohistological studies [23, 28] on adult penile nerves, both documenting increased ventrodorsal neural densities and one [28] reporting increased proximal intracavernous nNOS+ nerves and their reduction distally, suggesting these neural patterns are established early in ontogeny. Molecular mechanisms of axonal guidance in the developing human penis should now begin to be explored, and our fetal pan-TRK data suggest that epithelial-mesenchymal trophic (and possibly tropic) interactions via partly neurotrophins secreted by penile epithelia control nerve target invasion and terminal axonal branching. We identified a proportional relation between fetal preputial epithelial thickness and the underlying mesenchymal nerve density, very evident ventrally at 16 weeks, suggesting that epithelial thickness is somehow instrumental in determining preputial innervation patterns. We are currently working to disentangle specific neurotrophic and axonal guidance molecules implicated to present a clearer developmental picture of these phenomena. Although our study was not focused on age-related differences in corpuscular receptor densities and morphologies, we did observe that in the older specimens (>60 years) sensory corpuscles maintained relatively high levels in ventral compared to dorsal sections. We hypothesize that this may be



related to a differential neurotrophic support of sensory corpuscles across different penile skin regions.

The five histological levels of the adult prepuce with the central smooth muscle axis [57, 82] were clearly visible in our fetal specimens. We showed that the dense intricate preputial dartos

receives autonomic noradrenergic excitatory and nitergic presumably inhibitory innervation, but the denser neuromuscular supply observed with NSE and CD56 suggests other molecules are implicated in its regulation. The degree to which the functional properties of the preputial dartos fall between the two classical

**Fig. 6 Preputial smooth muscle and its dual autonomic innervation.** **A** is a low-magnification image for a general overview of  $\alpha$ -SMA distribution in this sagittal fetal penile section lateral to the urethra. This is the same specimen from Figs. 2A and 4. **B, C** are higher magnifications of the correspondent rectangles in **(A)** and **J** is more than 100  $\mu$ m apart from a region near the rectangle in **(F)**.  $\alpha$ -SMA+ dartoic smooth muscle formed a major constituent of the fetal **(A–C)** and adult **(D–K)** preputial pentalaminar structure, situated between thin bip epithelial stromal layers of the outer and inner prepuce. In fetuses, its initial proliferation revealed a finely fibrillar histological stratum, tightly compacted in the dorsal **(B)** and ventral **(C)** prepuce of this 16-week specimen, with no significant aggregation into bundles. At 20 weeks and older fetuses small smooth myocyte bundles were present and due to an increase in the extracellular matrix the compact dartos morphology in **(A–C)** changed to a more spread out appearance over the preputial mesenchyme. In the adult prepuce, the dartos appeared differentiated into an abundance of mature smooth muscle cells aggregated in relatively large fascicles configuring a more or less plexiform dartos layer, sympathetically **(F–I)** and parasympathetically **(J, K)** innervated. Autonomic fibers were in close contact with the basal lamina of myocytes, partially confined at myocyte deep or shallow invaginations, or at a few microns away from myocytes, thus creating a mixture of neuromuscular appositions. In some specimens, low-magnification images **(D)** revealed an overall annular orientation of dartoic bundles but in others, no such pattern could be discerned. In the upper right corner of **(E)** note a Pacinian corpuscle with slight  $\alpha$ -SMA positivity in the outermost capsular layers. In **(G–K)** note the abundance of TH+ and nNOS+ nerve bundles and the close association of autonomic elements with vascular and dartos smooth myocytes. TH and nNOS autonomic nerve profiles were restricted to subpapillary levels, suggesting autonomic regulation of papillary capillaries by different molecules. Scale bars: 0.5 mm **(A)**, 200  $\mu$ m **(B, C, E, H, I)**, 2 mm **(D, F)**, 600  $\mu$ m **(G)**, 300  $\mu$ m **(J)**, 100  $\mu$ m **(K)**.

extremes of multiunit or single-unit [84] smooth muscle is unknown. Being continuous with the scrotal and proximal penile dartos [82], the preputial dartos may hypothetically contract reflexively during erection tensing and stiffening penile skin, but how exactly these actions participate in erectile physiology and reflexes is an open question.

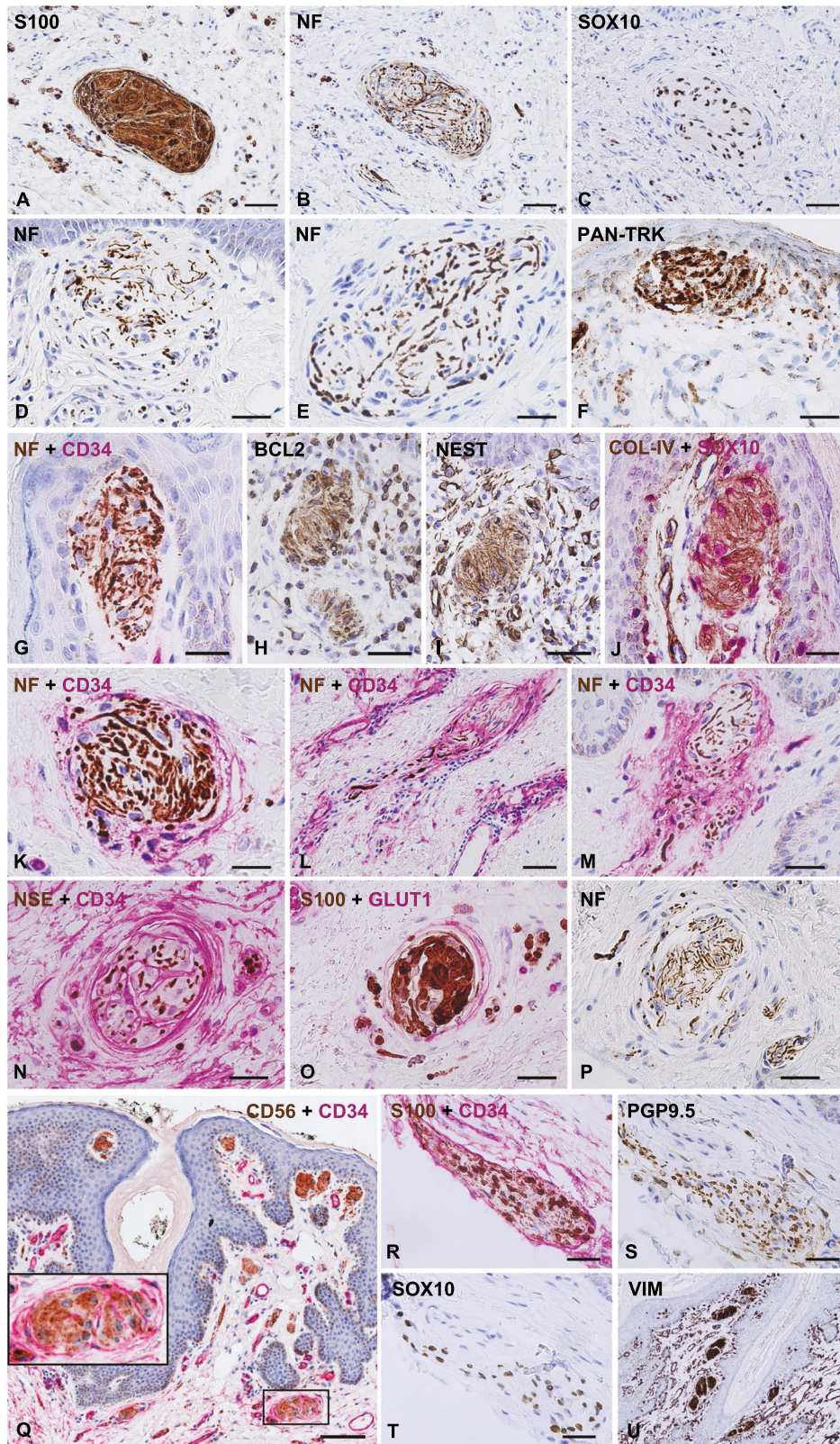
#### Circumcision and sexual sensation

In the fetal ages we studied, sagittal sections revealed that the prepuce represents the majority of the fetal penile integument (covering), but this may also be true for the adult penis [57, 85]. A recent cadaveric dissection study documented that the majority of the clitoral prepuce is clitoral shaft skin [86], and the penile and clitoral prepuces are homologous structures. Partial or total removal of the clitoral prepuce, primarily for cultural or religious reasons, is practiced in some societies and tends to be characterized, by its supporters, as a physically harmless procedure, largely due to a presumption that there are no functional consequences to such cutting (an idea that may be based on a similar presumption regarding penile circumcision as practiced in the same societies) [87]. Although the absence of a prominent clitoral dartos layer and the lack of circumferential clitoral skin are conspicuous differences between the clitoral and penile prepuce [57, 81], both have a rich supply of corpuscular receptors [59] and nNOS+ innervation. Insofar as the clitoral and penile prepuces are homologous, the results of the present study may call into question the presumption of harmlessness for clitoral circumcision, in the sense of a lack of potential functional consequences or risk of adverse sexual sensation. At the point of its terminal arborization, Kelling et al. [86] reported that the average diameter of the dorsal nerve of the adult clitoris measured 2 mm, indicating a substantial volume of branching from the main trunk of the nerve to innervate the clitoral glans and prepuce. Unlike the position of the dorsal penile nerve beneath Buck's fascia, Kelling et al. [86] also reported that the dorsal clitoral nerve may be more superficial, and knowledge of this neuroanatomy is crucial to preserve sexual sensation and function during female genital surgeries.

Regarding penile circumcision, there continues to be heated debate in the medical literature in three interrelated arenas: its prophylactic, sexual and ethical aspects. We have no interest in and will not be a part of these confrontations, but our findings allow us to address the issue of sexual sensation and function with no other interest than improving patient safety. As with any surgery, circumcision has a potential for adverse outcomes related to the acute effects of the procedure, which should not be overlooked. Permanent altered penile sensation [40] is a reported effect of adult circumcision whose overall frequency is not known, yet neural substrates of this perplexing symptom remain obscure.

In the case of neonatal circumcision, the long delay between the surgery itself and subsequent conscious awareness of penile sensation as such obscures the potential connection between the two phenomena. Regardless of technique, circumcision involves resection of a circumferential tissular segment of varying dimensions excised at different distances from the inferior border of the corona. This whole circumferential segment is richly innervated by somatosensory and autonomic fibers, as well as richly vascularized and muscularized. However, deep incisions and resections in subcoronal regions of increased neural density (i.e., regions located in the paths of circumcision incisions) provide a rational anatomical and surgical basis for the negative sensory alterations reported by a subgroup of men (representativeness unknown). Our immunohistological analyses plus data accumulated from the other studies here reviewed direct attention to the distal third of the ventral penile aspect for its increased nerve supply and erogenous potential. Other structural aspects may be relevant: in the adult penis all tissue planes are frequently described as thinner in this region and the tunica albuginea is inconspicuous or absent at the glans level [30, 88, 89]. The tunica albuginea of the corpus spongiosum at the shaft level is also thinner than the dorsal tunica albuginea and the epithelium of the frenular area may be thinner than the dorsal glans epithelium [30]. The corpus spongiosum itself is reported to be thinner in penectomy specimens in which the distal corpora cavernosa is located within the glans than in cases in which they end in the penile body [90]. Thus, a very dense nerve supply seems to be compressed into a shortage of ventral tissues. These structural features might plausibly and theoretically reduce tissue resistance to incisions facilitating unintentional increases in cutting depth, which may in turn compromise regions of increased neural density which supply the more superficial tissues with very rich nerve bundle and corpuscular innervation. Furthermore, due to its high vascularity and the tendency of frenular bleeding, aggressive cauterizations here might cause inadvertent nerve damage.

One circumcision technique [91] has been proposed to protect as much tissue as possible ventrally due to the sexual functions attributed to this region. Concerningly and antithetically to the former technique, the frenular area has been intentionally targeted during adult circumcision by some urologists [92] in the belief that its total and permanent denervation using monopolar current might be a definitive treatment for life-long premature ejaculation. These urologists concluded that their circumcision technique resulted in "a consistent reduction in penile sensitivity" and "is a strong weapon in the hands of urological surgeons, which must be used very carefully, as its effects on male sexuality can be devastating and irreversible if performed in the wrong patient. Thus, the caveat must be



‘do the right circumcision in the right patient using the correct surgical technique’” (p. 146 of reference [92]). To the extent that this type of circumcision may impair sexual function by denervating a neurologically permissive substrate through which sexual sensation enters the central nervous system, we agree

with Jannini [93] that denervation of the frenular region is a potentially dangerous intervention. The above quote also highlights that variations in circumcision technique likely factor into potential adverse outcomes in relation to penile sensation. The possibility that aggressive circumcisions performed with

**Fig. 7 Human adult preputial corpuscular receptors and their immunohistochemical profiles.** Our analyses of preputial innervation revealed highly organized, dense receptor arrays and a wide spectrum of corpuscular formations. Single immunohistochemistry: **A–C** depict a serially sectioned large, encapsulated, internally lobulated genital corpuscle with S100+ (**A**) and SOX10+ (**C**) Schwann cells and NF+ axonal profiles (**B**), positioned in the reticular dermis. **D** is a variety of non-encapsulated nerve formation consisting of axonal proliferations and Schwann cells arranged in no particular order. **E** is another encapsulated genital corpuscle composed of unmyelinated NF+ axons and Schwann cells. Serial sections (not shown) confirmed internal lobulation. **F** is a nerve formation with its long axis parallel to the epithelial surface and dense pan-TRK+ axons arranged between lamellar cells with peripherally located nuclei. No capsule is apparent. **H, I** are approximately 10 µm apart and show a Bcl-2+ and nestin+ corpuscle with similar staining patterns amid an inflammatory cell infiltrate. Serial sections (not shown) with CD34 revealed thin encapsulation. **P** shows a corpuscular receptor in the reticular dermis displaying a typical tangling of unmyelinated nerve amid non-myelinating Schwann cells. No internal lobulation or septation is evident. For **S, T** see below. **U** displays a receptor array typical of the ventral prepuce clustering a series of vimentin+ corpuscles, some lobulated. Double immunohistochemistry: **G** is a non-encapsulated papillary nerve formation displaying a dense, tightly packed NF+ unmyelinated axonal mass intimately abutting its dermal papilla. **J** is a Meissner corpuscle with SOX10+ nuclear staining of its lamellar cells and a COL-IV+ staining pattern identical to that of (**H, I**). Note endothelial COL-IV+ basal lamina staining of adjacent capillaries and SOX10+ adjacent melanocytic nuclei. **K** is a Krause corpuscle in the reticular dermis showing glomerularly arranged NF+ thickened axons, decorated by a thin CD34+ nest-like ensheathment. **L** displays a fusiform formation resembling a Ruffini corpuscle with NF+ axons and CD34+ condensations. **M** is a Meissner corpuscle with NF+ axons surrounded by a CD34+ flame-like stromal condensation, escorted by an adjacent smaller corpuscle. **N, O** depict a serially sectioned deep dermal receptor displaying CD34+ endoneurial ensheathment and internal septa (magenta in **N**) compartmentalizing NSE+ axonal profiles (brown in **N**), but also Glut-1+ (magenta in **O**) perineurial investment, an infrequent finding. Between the Glut-1+ perineurium and the surrounding dermis a connective tissue with a denser texture is apparent, which might have corresponded to epineurium. **Q** illustrates the general tendency of greater encapsulation of non-papillary corpuscles and lesser or absent encapsulation of papillary corpuscles. Inset is a higher magnification of the rectangular depicting a genital corpuscle with a CD34+ capsule emitting internal septa (magenta) and CD56+ non-myelinating Schwann cells (brown). **R–T** show a serially sectioned non-papillary corpuscle similar to (**L**), with S100+ (brown in **R**) and SOX10+ (brown in **T**) Schwann cells, a very thin CD34+ ensheathment (magenta in **R**) and PGP9.5+ axonal profiles (**S**). **D, E, P, U** correspond to cadaver specimens and all other images to fresh preputial specimens. Scale bars: 50 µm (**A–C, L, U**), 20 µm (**K**), 30 µm (**D–J, M–P, R–T**), 100 µm (**Q**).

improper surgical handling of ventral tissues might inadvertently lead to overlapping or partially overlapping effects to those described by Gallo et al. [92] is not implausible. Taking the sleeve technique as an example of surgical flexibility during circumcision, to the extent that this technique is of such versatility that it allows highly variable quantities of cutaneous and subcutaneous tissue to be excised directly from the penile body, and to the extent that the prepuce is still conceived by segments of the medical community as “just a small piece of skin”, we are concerned that aggressive circumcisions are intentionally or unintentionally being performed in pediatric and adult patients in the belief that “redundant” or “extra” tissue is being excised, or in the belief that “excessive sensitivity” is being reduced to augment ejaculatory latency time.

Macroscopic dissections [48] have claimed a paucity of ventral penile nerves potentially granting surgical license for more aggressive operations ventrally, but immunohistology is gold standard for verification of such results, which conflict with recent literature [23, 28, 29]. Added to this, anatomy textbooks [94] frequently portray the ventral aspect of the penis with no nerves or show only the scrotal distribution of the perineal nerve, a tendency that should be amended. Yang and Bradley's [48] inability to macroscopically identify longitudinal ventral nerves on the surface of the corpus spongiosum and the identification of these nerves by recent immunohistological studies [28, 29] may in part reflect differences between macroscopic and histological observations. Nevertheless, as Yang and Bradley's [48] dissections were performed after removal of the penile shaft skin and fascial layers, this also suggests the possibility that perineal nerves might have a more superficial or variable position. Thus, more research on the course and exact three-dimensional positions of the adult penile perineal nerves is warranted.

Perineal nerves also innervate the bulbospongiosus and ischiocavernosus muscles and pudendo-perineal somatic-somatic and pudendo-cavernosal somatic-autonomic spinal reflexes produce rigid erections [1]. The afferent arm of these reflex loops is mediated by perineal and dorsal nerves, both of which innervate penile skin including the prepuce. The dorsal nerve has been studied extensively by anatomical dissections, electrophysiology and immunohistochemistry. Its integrity is crucial for normal erectile and ejaculatory function and its role in male

sexual function is well established. Neuroanatomical and neurophysiological information about the perineal nerve is limited, which has restricted its analysis in relation to sexual function, but it also is important for sexual reflexes involved in initiation and maintenance of erection [47]. Perineal nerve stimulation in humans [47] and in a canine model [95] produced erection, and pathological reductions of ischiocavernosus and bulbospongiosus muscle contractility correlate with erectile dysfunction [96]. Insofar as circumcision carries a risk of decreased sexual function or altered penile sensation experienced as negative, these outcomes may be related to a potential interference with afferent drives of penile reflexes caused by deep incisions [23], aggressive subcutaneous resections, suture placements or cauterizations that compromise the innervation of the distal third of the ventral penile aspect, which is innervated by the perineal nerve and some dorsal nerve ramifications. Such a possibility is supported by our analyses of the relevant literature and our structural data. The sexual reflexes (discussed in our introduction) elicited in spinal cord-injured patients by vibratory or manual stimulation of the frenular area [32–34] also suggest this is somehow a region with special pro-erectile reflexive properties.

We recommend quantitative sensory testing and electrophysiological explorations of the whole ventral penile surface in patients reporting symptoms of severe and permanent penile sensory loss post-adult circumcision, including biothesiometry and evaluation of penile somatosensory evoked potentials. In addition, we advise that circumcision incisions should be made as superficially as is possible [97]. This will help reduce potential complaints of penile sensory loss (or other negative alterations). Electrocautery for controlling bleeding ventrally should also be approached with caution. Careful interrogations of these patients may determine whether there are specific, well-defined penile body regions where hypesthesia, numbness, and other sensory alterations are preferentially located, paying close attention to the special sexually responsive regions like the frenular area and adjacent ventral tissues.

#### Study limitations

Limitations of this study include (i) the small number of specimens, (ii) possible artifactual tissue modifications due to

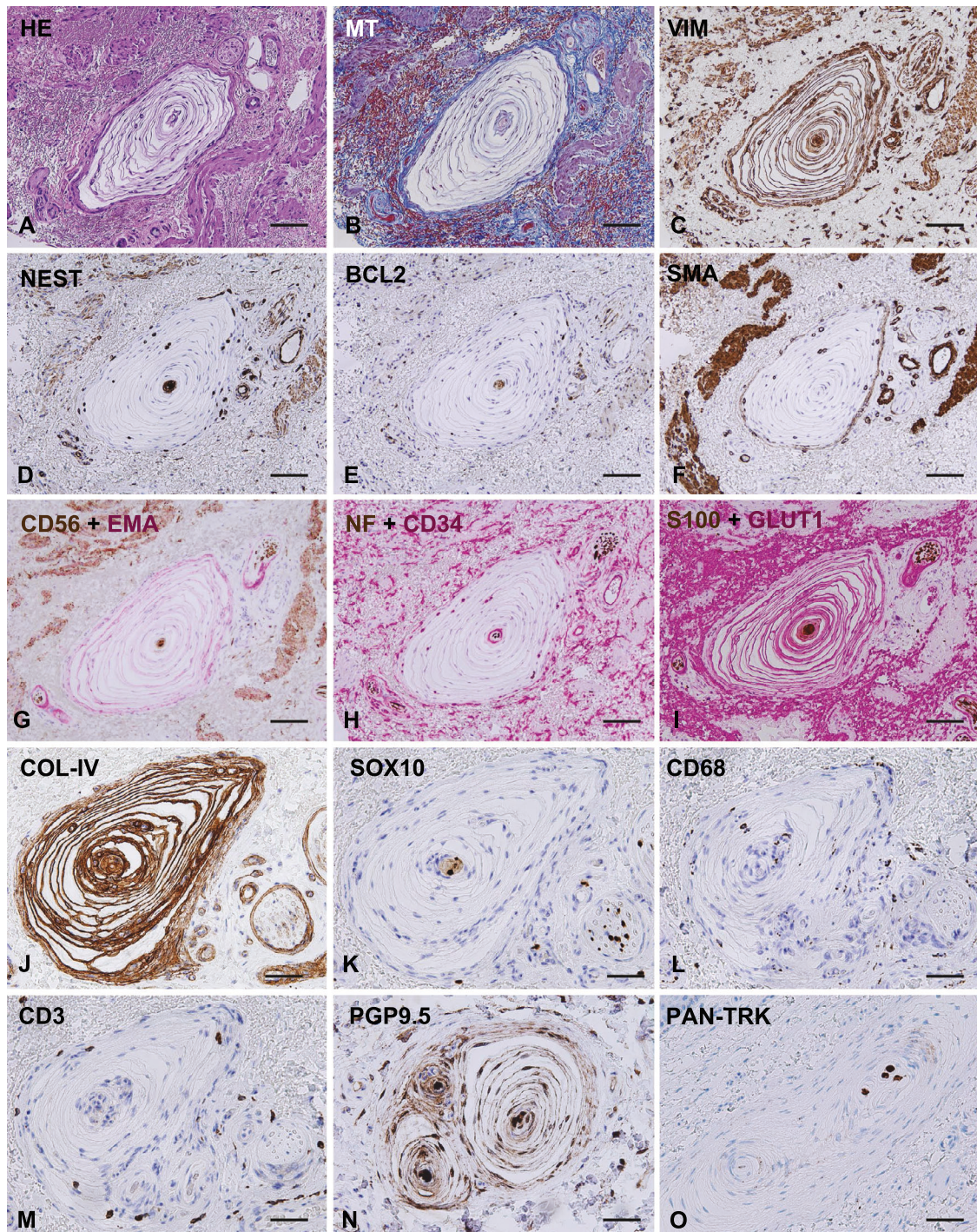


**Fig. 8 Immunohistochemical profile of a serially sectioned human preputial Pacinian corpuscle located deep in the dorsal dartos layer of a 68-year-old man.** HE (A) and MT (B) stains depict the same corpuscle as (C–M), but N displays a different Pacinian corpuscle from the same individual and O a Pacinian from a 32-year-old man. J–M are serial sections approximately 14  $\mu\text{m}$  apart from (I). Single immunohistochemistry: vimentin (C) and COL-IV (J) immunolabeled all Pacinian structural compartments except apparently the endoneurial intermediate layer. Nestin (D), Bcl-2 (E) and SOX10 (K) were expressed by the inner core Schwann cells, and  $\alpha$ -SMA (F) capsular immunoreactivity decorated this Pacinian corpuscle, suggestive of contractile properties. CD68 (L) and CD3 (M) immunodetected intracapsular macrophages and T-cells, respectively. PGP9.5 (N) and pan-TRK (O) immunostained inner core axons but PGP9.5 also the perineurial outer core. In N, a small paciniform structure is fused with two larger Pacinians of increasing size into a common capsule and in O, one Pacinian seems compartmentalized into several inner cores that partially share a common perineurial outer core. Such Pacinian complexes were not a rare occurrence. In the upper left corner of O, note the preputial epidermis, indicating the position of this Pacinian in the superficial reticular dermis. Double immunohistochemistry: EMA (magenta in G) and Glut-1 (magenta in I) immunolocalized in the perineurial outer core, CD56 (brown in G) and S100 (brown in I) in the inner core Schwann cells, and CD34 (magenta in H) in the endoneurial intermediate layer. Inner core axonal profiles were immunopositive for CD56 (note darker brown spots in G), NF (brown in H) and NSE (not shown). The outer core and capsule contained a vimentin+ (C), nestin+ (D),  $\alpha$ -SMA+ (in pericytes) (F), CD34+ (H) and COL-IV+ (J) capillary network. Except for capsular  $\alpha$ -SMA, these immunoreactivities were generally consistent across Pacinian corpuscles. Nerve and smooth muscle bundles, CD34+ dermal cells (H), blood vessels and Glut-1+ extravasated red blood cells (B, I) surround the corpuscle. For a clear and concise description of Pacinian structure see reference [38]. Scale bars: 100  $\mu\text{m}$  (A–I), 50  $\mu\text{m}$  (J–O).

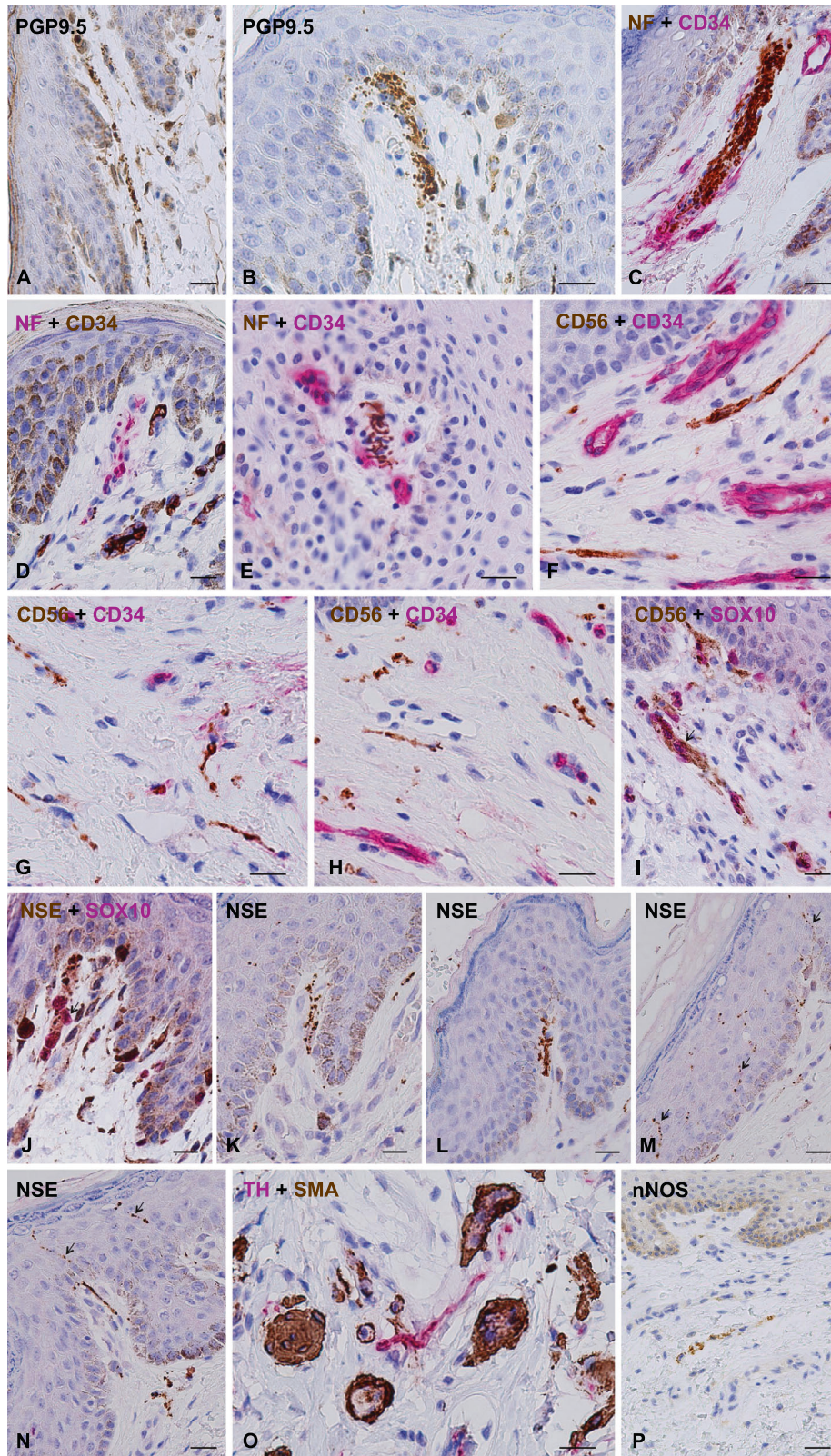


**Fig. 9 Human adult preputial FNEs and their immunohistochemical profiles.** Attention to detail was necessary to detect the abundance of these minute, delicate, but occasionally thick unmyelinated nerve fibers devoid of CD34+ associated cells (but see C). We were able to detect them in all histological strata with PGP9.5 (A, B), NF (C–E), CD56 (F–I), NSE (J–N), TH (O) and rarely nNOS (P), decorated or not with SOX10+ cells (arrows in I, J). In subpapillary levels it was often difficult to discern if they were true FNEs or isolated and solitary, exploratory preterminal fibers arising from small nerve fascicles and sectioned across their paths. TH+ and nNOS+ FNEs were absent in the papillary dermis, being restricted to deeper levels. Sometimes FNEs formed complicated spirals (E) whose three-dimensional character could be visualized in our 4- $\mu$ m-thick sections. These could have been very small corpuscles. Intraepithelial fibers were best detected with PGP9.5 (not shown) and NSE (arrows in M, N). Scale bars: 20  $\mu$ m (A–O), 40  $\mu$ m (P).

histological processing, (iii) absence of fetal penile transverse sections to confirm observations made in sagittal sections, (iv) use of preputial specimens with pathology, and (v) use of perfusion-fixed cadavers. S100+ nerve bundle densities were reduced in cadaver tissues compared to fresh preputial samples. We attribute this partly to reduced antigenicity of perfusion-fixed cadavers as not all our antibodies produced in these tissues the crisp and intense staining that was characteristic of the other specimens. Regarding the third limitation, we performed extensive serial section analyses of the fetal sagittal sections and thus have confidence in our observations. For the fourth limitation, our findings are in line with results from studies [25–27, 57, 61–63, 85, 97] using normal preputial specimens. In those preputial tissues with obvious inflammation included in our study, nerve bundles displayed a normal structure and distribution, immunoreactive patterns of neural tissue were preserved, and corpuscular receptors simply appeared amid inflammatory cell infiltrates (resulting in quite esthetic histological preparations, incidentally). The small specimen number limits the capacity to detect anatomical and histological variations. We tried to partly compensate for this limitation by exhausting paraffin blocks and analyzing large numbers of sections per specimen. This allowed us to document a remarkably rich nerve supply and corpuscular receptors of high complexity. Such complexities reminded us of observations attributed [98] to the Italian histologist Angelo Ruffini that between the more or less well-defined classical corpuscular receptors and FNEs there is an innumerable variety of transitional receptor types, making rigid classifications futile and creating a breeding ground for proliferative terminology.

## CONCLUSIONS

Our findings support a model of penile body innervation with higher cutaneous and subcutaneous nerve bundle and corpuscular densities in the distal third of the ventral aspect and a reduction in two directions perpendicular to each other: proximally following the longitudinal axis and dorsally perpendicular to the longitudinal gradient. These orthogonal nerve arrays might partly explain the specialized or heightened sexual sensations originating from the distal ventral shaft and may, moreover, have some explanatory value regarding post-circumcision negative penile sensory alterations reported by some men. This may also be the first study to demonstrate the dual autonomic neuromuscular and neurovascular innervation of the prepuce by TH+ and nNOS+ nerves. A proximodistal intracavernous autonomic fiber distribution with higher proximal levels was described in the adult penis by Diallo et al. [28], and here we provided the first evidence of this neural pattern in the fetal penis. This proximodistal gradient may in turn guarantee erectile rigidity and stability in the fixed, non-mobile triradiated penile root, supporting the pendulous penis during sexual intercourse [28]. A predominance of intracavernosal pillars within the distal corpora cavernosa nevertheless provides structural support and enhances erectile rigidity distally [99]. The analyses of penile innervation presented in this study provide a general anatomical and histological framework that may allow a better understanding of male sexual function and dysfunction. Studies are in progress in our laboratory to further test these observations and compare preputial and glans innervations in a larger fetal and fresh cadaveric series.

## DATA AVAILABILITY

Data supporting results of this study are available from the corresponding author on reasonable request.

## REFERENCES

- Tajkarimi K, Burnett AL. The role of genital nerve afferents in the physiology of the sexual response and pelvic floor function. *J Sex Med.* 2011;8:1299–312.
- Gollaher DL. Circumcision: a history of the world's most controversial surgery. New York: Basic Books; 2000.
- Glick L. Marked in your flesh: circumcision from ancient Judea to modern America. New York: Oxford University Press; 2005.
- Darby R. A surgical temptation: the demonization of the foreskin and the rise of circumcision in Britain. Chicago: University of Chicago Press; 2005.
- Fink KS, Carson CC, DeVellis RF. Adult circumcision outcomes study: effect on erectile function, penile sensitivity, sexual activity and satisfaction. *J Urol.* 2002;167:2113–6.
- Masood S, Patel HRH, Himpson RC, Palmer JH, Mufti GR, Sheriff MKM. Penile sensitivity and sexual satisfaction after circumcision: are we informing men correctly? *Urol Int.* 2005;75:62–6.
- Kim D, Pang M-G. The effect of male circumcision on sexuality. *BJU Int.* 2007;99:619–22.
- Frisch M, Lindholm M, Grønbaek M. Male circumcision and sexual function in men and women: a survey-based, cross-sectional study in Denmark. *Int J Epidemiol.* 2011;40:1367–81.
- Bronselaer GA, Schober JM, Meyer-Bahlburg HFL, T'Sjoen G, Vlietinck R, Hoebeke PB. Male circumcision decreases penile sensitivity as measured in a large cohort. *BJU Int.* 2013;111:820–7.
- Dias J, Freitas R, Amorim R, Espiridião P, Xambre L, Ferraz L. Adult circumcision and male sexual health: a retrospective analysis. *Andrologia.* 2014;46:459–64.
- Hammond T. A preliminary poll of men circumcised in infancy or childhood. *BJU Int.* 1999;83:85–92.
- Hammond T, Carmack A. Long-term adverse outcomes from neonatal circumcision reported in a survey of 1,008 men: an overview of health and human rights implications. *Int J Hum Rights.* 2017;21:189–218.
- Hammond T, Reiss MD. Antecedents of emotional distress and sexual dissatisfaction in circumcised men: previous findings and future directions—comment on Bossio and Pukall (2017). *Arch Sex Behav.* 2018;47:1319–20.
- Tian Y, Liu W, Wang JZ, Wazir R, Yue X, Wang KJ. Effects of circumcision on male sexual functions: a systematic review and meta-analysis. *Asian J Androl.* 2013;15:662.
- Bossio JA, Pukall CF, Steele S. A review of the current state of the male circumcision literature. *J Sex Med.* 2014;11:2847–64.
- Bossio JA, Pukall CF, Steele S. Response to: the literature supports policies promoting neonatal male circumcision in N. America. *J Sex Med.* 2015;12:1306–7.
- Earp BD, Darby R. Circumcision, sexual experience, and harm. *U Penn J Int Law.* 2017;37:1–56.
- Deacon M, Muir G. What is the medical evidence on non-therapeutic child circumcision? *Int J Impot Res.* 2022. <https://doi.org/10.1038/s41443-021-00502-y>
- Wodwaski N, Munyan K. As nurses, are we meeting the unique needs of the intact client? *J Spec Pediatr Nurs.* 2022;27:e12356 <https://doi.org/10.1111/jspn.12356>
- Malhotra NR, Rosoklija I, Shannon R, D'Oro A, Liu DB. Frequency and variability of advice given to parents on care of the uncircumcised penis by pediatric residents: a need to improve education. *Urology.* 2020;136:218–24.
- Nelson ED. Penile anomalies and circumcision. In: Mattei P, Nichol P, Rollins II M, Muratore C, editors. *Fundamentals of pediatric surgery.* 2nd ed. Cham: Springer; 2017. p. 711–24.
- Benoit G, Droupy S, Quillard J, Paradis V, Giuliano F. Supra and infrallevator neurovascular pathways to the penile corpora cavernosa. *J Anat.* 1999;195:605–15.
- Jang HS, Hinata N, Cho KH, Bando Y, Murakami G, Abe S-I. Nerves in the cavernous tissue of the glans penis: an immunohistochemical study using elderly donated cadavers. *J Anat Soc India.* 2017;66:91–6.
- Winkelmann R. *Nerve endings in normal and pathologic skin.* Springfield: Charles C Thomas Publisher; 1960.
- Pérez Casas A, Vega Álvarez J, López Muñoz A, Romo Hidalgo E, Suárez Garnacho S, Bengoechea González E. [Microscopic innervation of the penis. I. Prepuce and glans penis]. *Arch Esp Urol.* 1988;41:1–7.
- Moldwin R, Valderrama E. Nerve distribution patterns within prepuce tissue: clinical applications in penile nerve blocks. *Anesth Analg.* 1990;70:S270. (abstract)
- Malkoc E, Ates F, Tekeli H, Kurt B, Turker T, Basal S. Free nerve ending density on skin extracted by circumcision and its relation to premature ejaculation. *J Androl.* 2012;33:1263–7.
- Diallo D, Zaitouna M, Alsaid B, Quillard J, Ba N, Allodji RS, et al. The visceromotor and somatic afferent nerves of the penis. *J Sex Med.* 2015;12:1120–7.
- Flochlay M, Diallo D, Bessede T, Prudhomme M, Costa P, Kharlamov E, et al. Receptors and sensory nerve pathways of the penis: a three dimensional

- computer assisted anatomical dissection (3DCAAD). *Eur Urol Suppl.* 2019;18:e1253. (abstract 927)
30. Halata Z, Munger BL. The neuroanatomical basis for the protopathic sensibility of the human glans penis. *Brain Res.* 1986;371:205–30.
  31. Cunha GR, Sinclair A, Cao M, Baskin LS. Development of the human prepuce and its innervation. *Differentiation.* 2020;111:22–40.
  32. Kuhn RA. Functional capacity of the isolated human spinal cord. *Brain.* 1950;73:1–51.
  33. Pryor JL, LeRoy SC, Nagel TC, Hensleigh HC. Vibratory stimulation for treatment of anejaculation in quadriplegic men. *Arch Phys Med Rehabil.* 1995;76:59–64.
  34. Ellis RG. The corona-frenulum trigger. *Sex Disabil.* 1980;3:50–6.
  35. Bossio JA, Pukall CF, Steele SS. Examining penile sensitivity in neonatally circumcised and intact men using quantitative sensory testing. *J Urol.* 2016;195:1848–53.
  36. Sorrells ML, Snyder JL, Reiss MD, Eden C, Milos MF, Wilcox N, et al. Fine-touch pressure thresholds in the adult penis. *BJU Int.* 2007;99:864–9.
  37. García-Mesa Y, García-Piqueras J, Cobo R, Martín-Cruces J, Suazo I, García-Suárez O, et al. Sensory innervation of the human male prepuce: Meissner's corpuscles predominate. *J Anat.* 2021;239:892–902.
  38. Cobo R, García-Piqueras J, Cobo J, Vega JA. The human cutaneous sensory corpuscles: an update. *J Clin Med.* 2021;10:227.
  39. Cobo R, García-Piqueras J, García-Mesa Y, Feito J, García-Suárez O, Vega JA. Peripheral mechanobiology of touch—studies on vertebrate cutaneous sensory corpuscles. *Int J Mol Sci.* 2020;21:6221.
  40. Reynard J, Brewster S, Biers S, Neal N. *Oxford handbook of urology.* 4th ed. Oxford: Oxford University Press; 2019. p. 785.
  41. Schober JM, Meyer-Bahlburg HF, Dolezal C. Self-ratings of genital anatomy, sexual sensitivity and function in men using the “Self-Assessment of Genital Anatomy and Sexual Function, Male” questionnaire. *BJU Int.* 2009;103:1096–103.
  42. McKenna K. SSI Grand Master Lecture 3 The brain is the master organ in sexual function: central nervous system control of male and female sexual function. *Int J Impot Res.* 1999;11:548–555.
  43. Fahmy M. Bleeding complications. In: Fahmy M, editor. *Complications in male circumcision.* St. Louis: Elsevier; 2019. p. 65–72.
  44. Yucel S, Baskin LS. Identification of communicating branches among the dorsal, perineal and cavernous nerves of the penis. *J Urol.* 2003;170:153–8.
  45. Yucel S, Baskin L. The detailed topographical anatomy of the perineal nerves on the penis and perineum: surgical Implications. *Eur Urol Suppl.* 2004;3:106.
  46. Yucel S, Baskin LS. Neuroanatomy of the male urethra and perineum. *BJU Int.* 2003;92:624–30.
  47. Uchio EM, Yang CC, Kromm BG, Bradley WE. Cortical evoked responses from the perineal nerve. *J Urol.* 1999;162:1983–6.
  48. Yang CC, Bradley WE. Peripheral distribution of the human dorsal nerve of the penis. *J Urol.* 1998;159:1912–6.
  49. Yang CC, Bradley WE. Neuroanatomy of the penile portion of the human dorsal nerve of the penis. *Br J Urol.* 1998;82:109–13.
  50. Gilbert-Barness E, Debich-Spicer D. *Embryo and fetal pathology: color Atlas with ultrasound correlation.* Cambridge: Cambridge University Press; 2004.
  51. García-Mesa Y, Cárcaba L, Coronado C, Cobo R, Martín-Cruces J, García-Piqueras J, et al. Glans clitoridis innervation: PIEZO2 and sexual mechanosensitivity. *J Anat.* 2021;238:446–54.
  52. Van de Velde TH. *Ideal marriage: its physiology and technique.* London: William Heinemann Medical Books; 1940.
  53. Zwang G. *La Fonction Érotique.* Paris: Éditions Robert Laffont; 1972.
  54. Young J. *An introduction to the study of man.* Oxford: Oxford University Press; 1974.
  55. Crooks R, Baur K. *Our sexuality.* 11th ed. Belmont: Wadsworth Cengage Learning; 2011.
  56. Hsu G-L, Liu S-P. Penis structure. In: Skinner MK, editor. *Encyclopedia of reproduction. Volume 1: male reproduction.* 2nd ed. Kidlington: Academic Press; 2018. p. 357–66.
  57. Cold CJ, Taylor JR. The prepuce. *BJU Int.* 1999;83:34–44.
  58. Winkelmann RK. The cutaneous innervation of human newborn prepuce. *J Invest Dermatol.* 1956;26:53–67.
  59. Seto H. *Studies on the sensory innervation (human sensibility).* 2nd ed. Springfield: Charles C Thomas Publisher; 1963.
  60. Georgiadis JR, Kringelbach ML. Intimacy and the brain: lessons from genital and sexual touch. In: Olausson H, Wessberg J, Morrison I, McGlone F, editors. *Affective touch and the neurophysiology of CT afferents.* New York: Springer; 2016. p. 301–21.
  61. Bourlond A, Winkelmann R. [The innervation of the prepuce of the newborn infant]. *Arch Belges Dermatol Syphiligr.* 1965;21:139–53.
  62. Chiarodo AJ. Fine structure of eight day human prepuce. *Anat Rec.* 1966;154:330.
  63. Bischoff A. Skin receptors of the human prepuce. In: Rohen JW, editor. *Functional morphology of receptor cells.* Mainz: Akademie der Wissenschaften und der Literatur; 1978. p. 64–87.
  64. Gratzl M, Langley K, editors. *Markers for neural and endocrine cells: molecular and cell biology, diagnostic applications.* New York: VCH Publishers; 1991.
  65. Mountcastle VB. *The sensory hand: neural mechanisms of somatic sensation.* Cambridge: Harvard University Press; 2005. p. 109.
  66. Díaz-Flores L, Gutiérrez R, García M, Gayoso S, Gutiérrez E, Carrasco JL. Telocytes in the normal and pathological peripheral nervous system. *Int J Mol Sci.* 2020;21:4320.
  67. Macklin WB, Rasband MN. Formation and maintenance of myelin. In: Brady ST, Siegel GJ, Albers RW, Price DL, editors. *Basic neurochemistry: principles of molecular, cellular, and medical neurobiology.* 8th ed. New York: Academic Press; 2012. p. 569–81.
  68. Lindsay RM. The role of neurotrophic factors in functional maintenance of mature sensory neurons. In: Scott SA, editor. *Sensory neurons: diversity, development, and plasticity.* New York: Oxford University Press; 1992. p. 404–20.
  69. García-Piqueras J, García-Mesa Y, Cárcaba L, Feito J, Torres-Parejo I, Martín-Biedma B, et al. Ageing of the somatosensory system at the periphery: age-related changes in cutaneous mechanoreceptors. *J Anat.* 2019;234:839–52.
  70. Saxod R. Ontogeny of the cutaneous sensory organs. *Microsc Res Tech.* 1996;34:313–33.
  71. Sieber-Blum M, editor. *Neural crest stem cells: breakthroughs and applications.* Singapore: World Scientific; 2012.
  72. Purpura V, Bondioli E, Cunningham EJ, Luca GDE, Capirossi D, Nigrisoli E, et al. The development of a decellularized extracellular matrix-based biomaterial scaffold derived from human foreskin for the purpose of foreskin reconstruction in circumcised males. *J Tissue Eng.* 2018;9:2041731418812613.
  73. Yucel S, De Souza A, Baskin LS. Neuroanatomy of the human female lower urogenital tract. *J Urol.* 2004;172:191–5.
  74. Schober J, Cooney T, Pfaff D, Mayoglu L, Martín-Alguacil N. Innervation of the labia minora of prepubertal girls. *J Pediatr Adolesc Gynecol.* 2010;23:352–7.
  75. Donadio V, Incensi A, Vacchiano V, Infante R, Magnani M, Liguori R. The autonomic innervation of hairy skin in humans: an in vivo confocal study. *Sci Rep.* 2019;9:1–7.
  76. Ruocco I, Cuello AC, Parent A, Ribeiro-Da-Silva A. Skin blood vessels are simultaneously innervated by sensory, sympathetic, and parasympathetic fibers. *J Comp Neurol.* 2002;448:323–36.
  77. Hosaka F, Yamamoto M, Cho KH, Jang HS, Murakami G, Abe S. Human nasociliary nerve with special reference to its unique parasympathetic cutaneous innervation. *Anat Cell Biol.* 2016;49:132–7.
  78. Alsaib B, Moszkowicz D, Peschard F, Bessedé T, Zaitouna M, Karam I, et al. Autonomic-somatic communications in the human pelvis: computer-assisted anatomic dissection in male and female fetuses. *J Anat.* 2011;219:565–73.
  79. Kozacioglu Z, Vatanserver H, Onal T, Kutlu N, Ozel F, Gunlusoy B, et al. Histologic and physiologic analysis of the relationship between the dorsal nerve of the penis and the corpus cavernosum on a rat model. A complementary pathway on the innervation of penile erection? *Neurourol Urodyn.* 2022;41:188–94.
  80. Kozacioglu Z, Kiray A, Ergur I, Zeybek G, Degirmenci T, Gunlusoy B. Anatomy of the dorsal nerve of the penis, clinical implications. *Urology.* 2014;83:121–5.
  81. Van der Putte SCJ. The development of the perineum in the human: a comprehensive histological study with a special reference to the role of the stromal components. Vol. 177. Berlin: Springer Science & Business Media; 2005.
  82. Velazquez EF, Barreto JE, Cañete-Portillo S, Cubilla AL. *Penis and distal urethra.* In: Mills S, editor. *Histology for pathologists.* 5th ed. Philadelphia: Wolters Kluwer; 2019. p. 1009–28.
  83. Kaneko S, Bradley WE. Penile electrodiagnosis: penile peripheral innervation. *Urology.* 1987;30:210–12.
  84. Christ GJ, Barr L. The neural control of smooth muscle. In Barr L, Christ GJ, editors. *Advances in organ biology.* Vol. 8. Stamford, CT: JAI Press; 2000. p. 345–95.
  85. Taylor JR, Lockwood AP, Taylor AJ. The prepuce: specialized mucosa of the penis and its loss to circumcision. *Br J Urol.* 1996;77:291–5.
  86. Kelling JA, Erickson CR, Pin J, Pin PG. Anatomical dissection of the dorsal nerve of the clitoris. *Aesthet Surg J.* 2020;40:541–7.
  87. Rashid A, Iguchi Y, Afiqah SN. Medicalization of female genital cutting in Malaysia: a mixed methods study. *PLoS Med.* 2020;17:e1003303.
  88. Palminteri E. Anatomy of the male urethra. In: Austoni E, editor. *Atlas of reconstructive penile surgery.* Pisa: Pacini Editore Medicina; 2010. p. 29–40.
  89. Montorsi F. Penile anatomy and the pathophysiology of erectile dysfunction. In: Austoni E, editor. *Atlas of reconstructive penile surgery.* Pisa: Pacini Editore Medicina; 2010. p. 41–51.
  90. Cubilla AL, Piris A, Pfannl R, Rodriguez I, Agüero F, Young RH. Anatomic levels: important landmarks in penectomy specimens: a detailed anastomotic and

- histologic study based on examination of 44 cases. *Am J Surg Pathol.* 2001;25:1091–4.
91. Shenoy SP, Marla PK, Sharma P, Bhat N, Rao AR. Frenulum sparing circumcision: step-by-step approach of a novel technique. *J Clin Diagn Res.* 2015;9:PC01–PC03.
  92. Gallo L. The prevalence of an excessive prepuce and the effects of distal circumcision on premature ejaculation. *Arab J Urol.* 2017;15:140–7.
  93. Jannini E. Re: The role of short frenulum and the effects of frenulectomy on premature ejaculation. *Eur Urol.* 2010;57:1119–20.
  94. Moore KL, Dalley AF, Agur AMR. *Clinically oriented anatomy.* 8th ed. Philadelphia: Wolters Kluwer; 2018.
  95. Shafik A. Perineal nerve stimulation: role in penile erection. *Int J Impot Res.* 1997;9:11–16.
  96. Colpi GM, Negri L, Nappi RE, China B, Colpi DGM. Perineal floor efficiency in sexually potent and impotent men. *Int J Impot Res.* 1999;11:153–7.
  97. Cakici OU, Pulular AG, Canakli F. Nerve-sparing circumcision: myth or reality? *J Pediatr Urol.* 2021;17:257–e1.
  98. Melzack R, Wall PD. On the nature of cutaneous sensory mechanisms. *Brain.* 1962;85:331–56.
  99. Brock G, Hsu G-L, Nunes L, Von Heyden B, Lue TF. The anatomy of the tunica albuginea in the normal penis and Peyronie's disease. *J Urol.* 1997;157:276–81.
  100. Chetty R, Cooper K, Gown AM. *Leong's manual of diagnostic antibodies for immunohistology.* 3rd ed. Cambridge: Cambridge University Press; 2016.
  101. Smoller BR. *Practical immunopathology of the skin.* New Jersey: Humana Press; 2010.
  102. True L, editor. *Atlas of diagnostic immunohistopathology.* New York: Gower Medical Publishing; 1990.
  103. Roche Tissue Diagnostics. VENTANA pan-TRK (EPR17341) Assay: Package Insert 1017533EN Rev A. [https://www.rochebiomarkers.be/content/media/Files/Bijlsuiter\\_790-702610175333EN.pdf](https://www.rochebiomarkers.be/content/media/Files/Bijlsuiter_790-702610175333EN.pdf). Accessed 3 Nov 2021.
  104. Calavia M, Viña E, Menéndez-González M, López-Muñiz A, Alonso-Guervós M, Cobo J, et al. Evidence of nestin-positive cells in the human cutaneous Meissner and Pacinian corpuscles. *CNS Neurol Disord Drug Targets.* 2012;11:869–77.
  105. Sjöstrand NO, Klinge E. Nitric oxide and the neural regulation of the penis. In: Vincent S, editor. *Nitric oxide in the nervous system.* London: Academic Press; 1995. p. 281–306.
  106. Arvidsson U, Riedl M, Elde R, Meister B. Vesicular acetylcholine transporter (VACht) protein: a novel and unique marker for cholinergic neurons in the central and peripheral nervous systems. *J Comp Neurol.* 1997;378:454–67.
  107. Rouvière H, Delmas A. *Anatomie humaine – descriptive, topographique et fonctionnelle (Tome 2, Tronc).* 15th ed. Paris: Masson; 2002. p. 614.
  108. McGrath K. The frenular delta: a new preputial structure. In: Denniston G, Hodges F, Milos M, editors. *Understanding circumcision: a multi-disciplinary approach to a multi-dimensional problem.* Boston: Springer; 2001. p. 199–206.
  109. McCammon KA, Zuckerman JM, Jordan GH. Surgery of the penis and urethra. In: Wein AJ, Kavoussi LR, Partin AW, Peters CA, editors. *Campbell-Walsh urology.* 11th ed. Philadelphia: Elsevier; 2016. p. 915.
  110. MacLennan GT. *Hinman's Atlas of urosurgical anatomy.* 2nd ed. Philadelphia: Elsevier Saunders; 2012. p. 323.
  111. Galiwango RM, Yegorov S, Joag V, Prodger J, Shahabi K, Huibner S, et al. Characterization of CD4+ T cell subsets and HIV susceptibility in the inner and outer foreskin of Ugandan men. *Am J Reprod Immunol.* 2019;82:e13143.
  112. Dinh MH, Hirbod T, Kigozi G, Okocha EA, Cianci GC, Kong X, et al. No difference in keratin thickness between inner and outer foreskins from elective male circumcisions in Rakai, Uganda. *PLoS One.* 2012;7:e41271.

## ACKNOWLEDGEMENTS

We would like to thank the anonymous reviewers for providing detailed and valuable feedback.

## AUTHOR CONTRIBUTIONS

AC-E, TG-C, RG and LG-C designed the study, interpreted results, and wrote the manuscript. AC-E, MG-C, MO-A and JS-Q recruited material. AC-E, MG-C, MO-A, HG, TG-C, RG, JS-Q and LG-C performed histopathological and immunohistochemical analyses. All authors revised and approved the manuscript.

## COMPETING INTERESTS

The authors declare no competing interests.

## ADDITIONAL INFORMATION

**Correspondence** and requests for materials should be addressed to Alfonso Cepeda-Emiliani.

**Reprints and permission information** is available at <http://www.nature.com/reprints>

**Publisher's note** Springer Nature remains neutral with regard to jurisdictional claims in published maps and institutional affiliations.